Supporting Information

Biomass-derived substrates hydrogenation over Rhodium Nanoparticles Supported on Functionalized Mesoporous Silica

Israel T. Pulido-Díaz [a,b], Draco Martínez [a], Karla P. Salas-Martin [a], Benjamín Portales-Martínez [d], Antonio Reina [a], Dominique Agustín [b,c], Itzel Guerrero-Ríos [a]*

[a] Departamento de Química Inorgánica y Nuclear, Facultad de Química, UNAM, Circuito Escolar S/N, Coyoacán, Cd. Universitaria, 04510 Ciudad de México, México.

[b] Centre National de la Recherche Scientifique (CNRS), Laboratoire de Chimie de Coordination (LCC), Université de Toulouse, UPS, INPT, 205, route de Narbonne, 31077 Toulouse, France

[c] Université de Toulouse, IUT P. Sabatier, Département de Chimie, Av. G. Pompidou, BP 20258, 81104 Castres CEDEX, France

[d] CONACYT, Centro de Investigación en Ciencia Aplicada y Tecnología Avanzada, Laboratorio Nacional de Conversión y Almacenamiento de Energía, Instituto Politécnico Nacional, Calzada Legaría 694, Col. Irrigación, Ciudad de México, 11500, México

TABLE OF CONTENTS

A. Infrared spectra

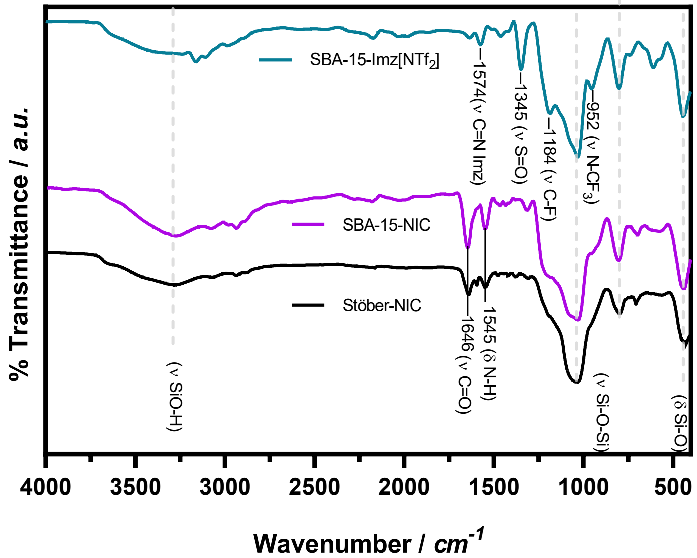

Figure S1. FTIR (ATR) spectra of functionalized SBA-15 based materials and Stöber silica.

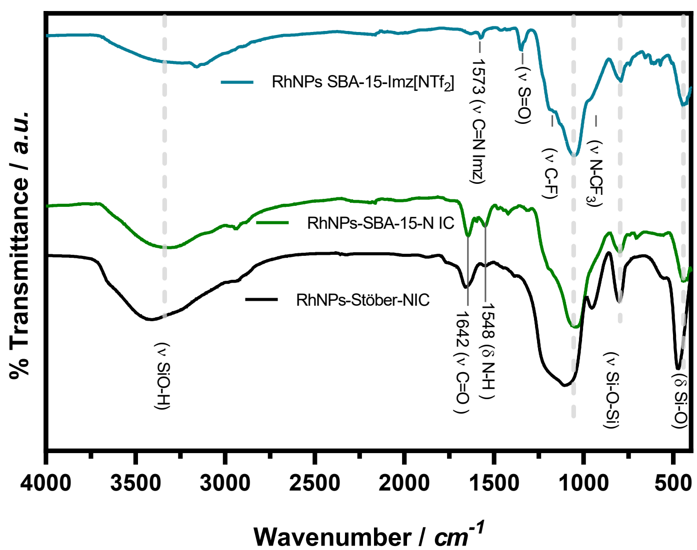

Figure S2. FTIR (ATR) of RhNPs supported on functionalized SBA-15 and Stöber silica

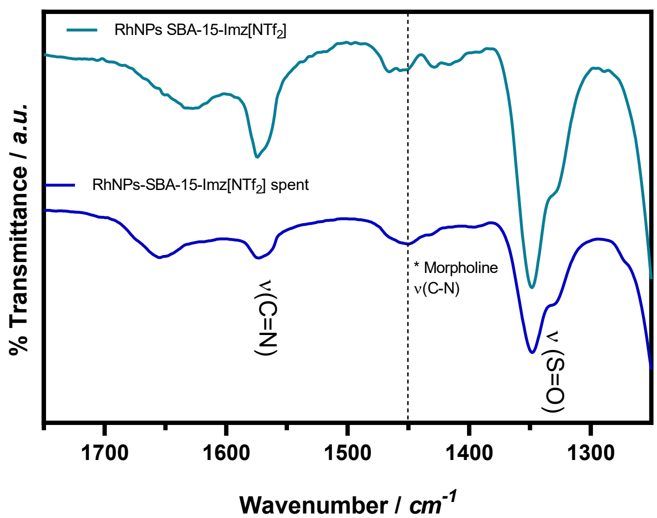

Figure S3. FTIR (ATR) of RhNPs@SBA-15-Imz [NTf_2] before and after phenol reductive amination in 1750-1250 cm^{-1}region.

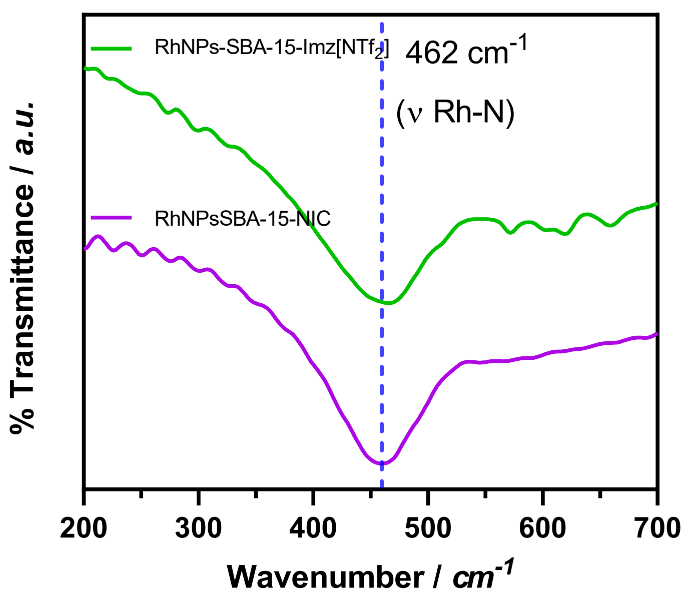

Figure S4. Far infrared spectra of RhNPs supported on functionalized SBA-15

B. TGA thermograms

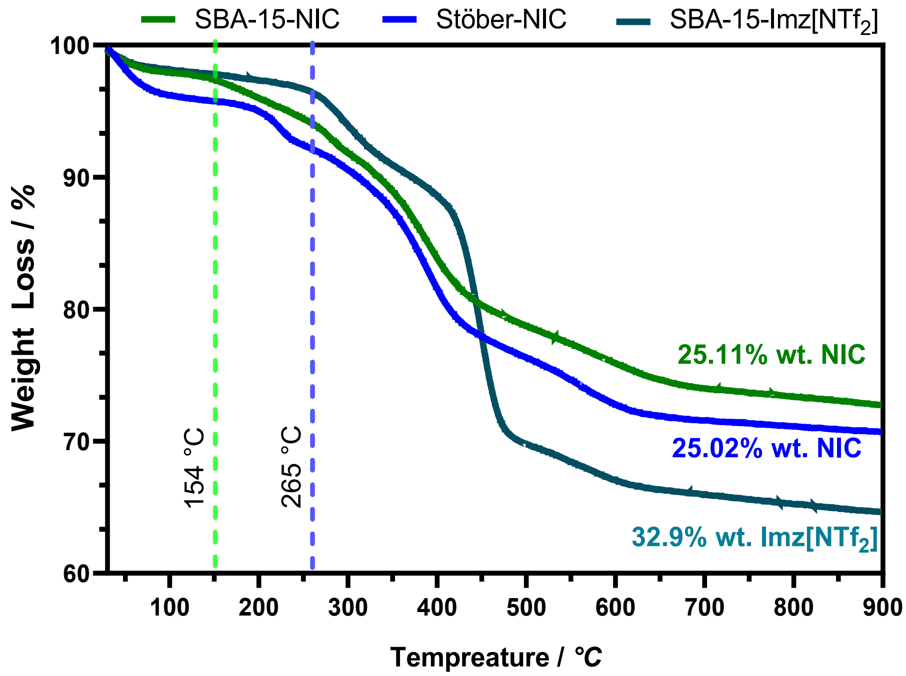

Figure S5. TGA curve of functionalized SBA-15 and Stöber silica

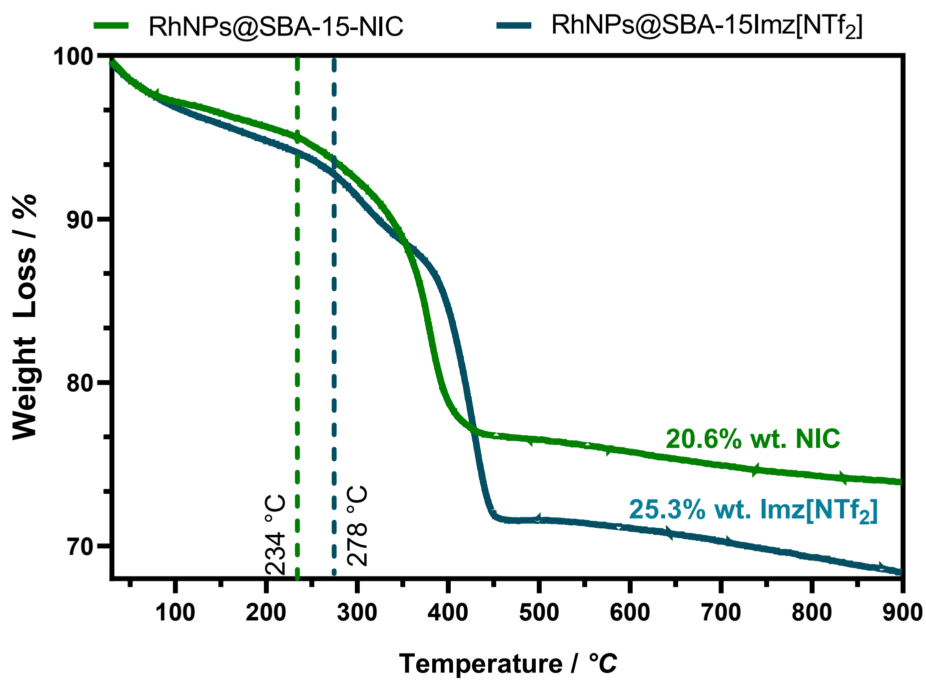

Figure S6. TGA curve of RhNPs supported in functionalized SBA-15.

C. PXRD data

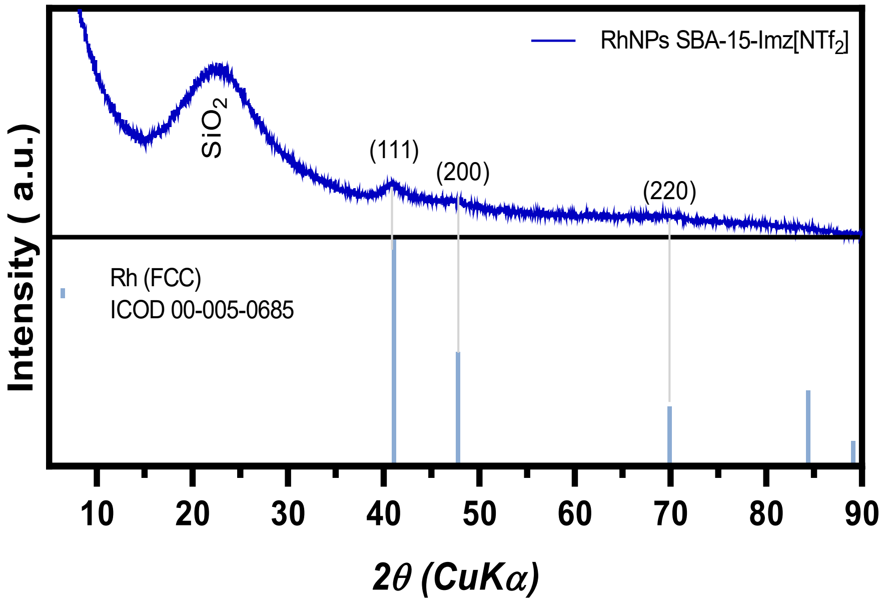

Figure S7. PXRD of RhNPs@SBA-15-Imz[NTf_2].

D. ^{29}Si NMR deconvolution data

Table S1. Relative concentration of T^n and Q^n sites obtained from ^{29}Si UDEFT spectra.

Material	^{29}Si-UDEFT-MAS[a]						φ ratio	% of silane Grafting[b]	% of Silanols (Si-OH)[b]	Grafting density (mmol g^{-1})[c]	BET Surface area (m^2g^{-1})	Surface coverage (molecules nm^{-2})
	T^1	T^2	T^3	Q^2	Q^3	Q^4						
SBA-15-Imz [NTf_2]	0.5	5.2	5.7	6.6	16.9	65.2	0.49	11.4	23.5	1.1	279	2.4
SBA-15-NIC	1.4	7.6	3.9	1.8	22.2	63.1	0.53	12.9	24.0	2.1	328	3.9

a) Percentage Area after deconvolution of ^{29}Si NMR spectrum. b) Determined based on the relative concentrations of T^n and Q^n. c) Determined by E.A and TGA.

E. [13]C CP-MAS Spactra

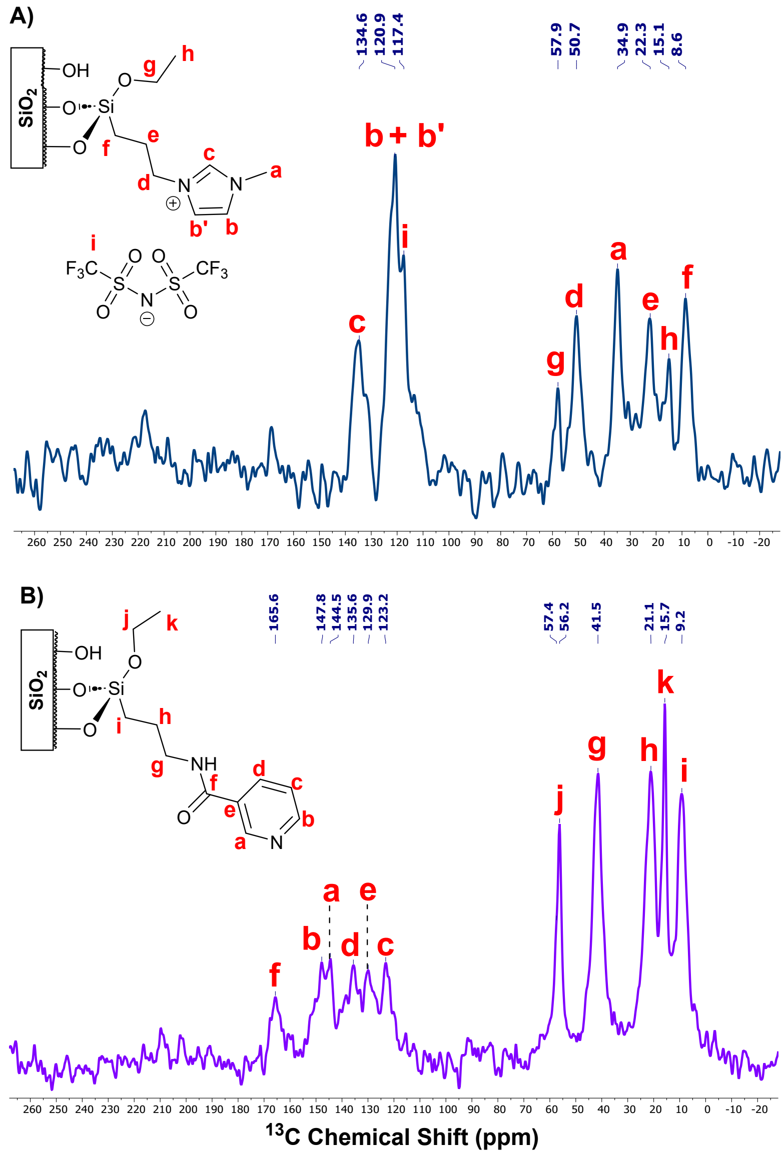

Figure S8. Solid [13]C CP-MAS NMR spectrum of SBA-15-Imz[NTf_2] (A), and SBA-15-NIC (B)

F. Nitrogen sorption/desorption isotherms at 77 K of MMS

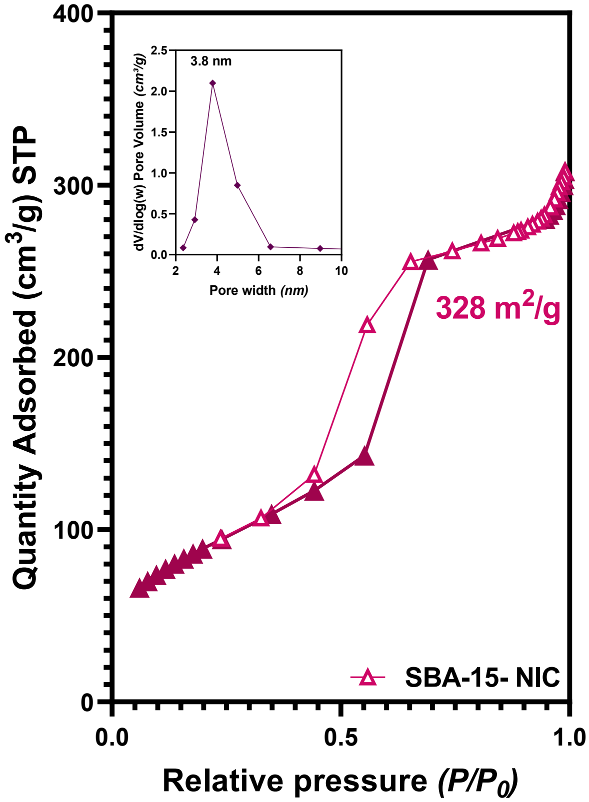

Figure S9. Adsorption-desorption isotherms of functionalized SBA-15 with pore size.

Table S2 BET isotherms analysis of functionalized silicas.

Entry	Material	S_{BET} ($m^2 g^{-1}$)[a]	Pore width[b] (nm)
1	**SBA-15**	902	5.7
2	**SBA-15 Imz[NTf$_2$]**	279	5.4.
3	**SBA-15 NIC**	328	3.8
4	**RhNPs@ SBA-15 Imz[NTf$_2$]**	211	5.4

[a] Calculated using Brunauer–Emmett– Teller (BET) model on the adsorption branch in the range of relative pressure (P/Po) from 0.06 to 0.196.

[b] Calculated using the BJH model for cylindrical pores

G. TEM and SEM micrographs with EDX analysis of pristine SBA-15

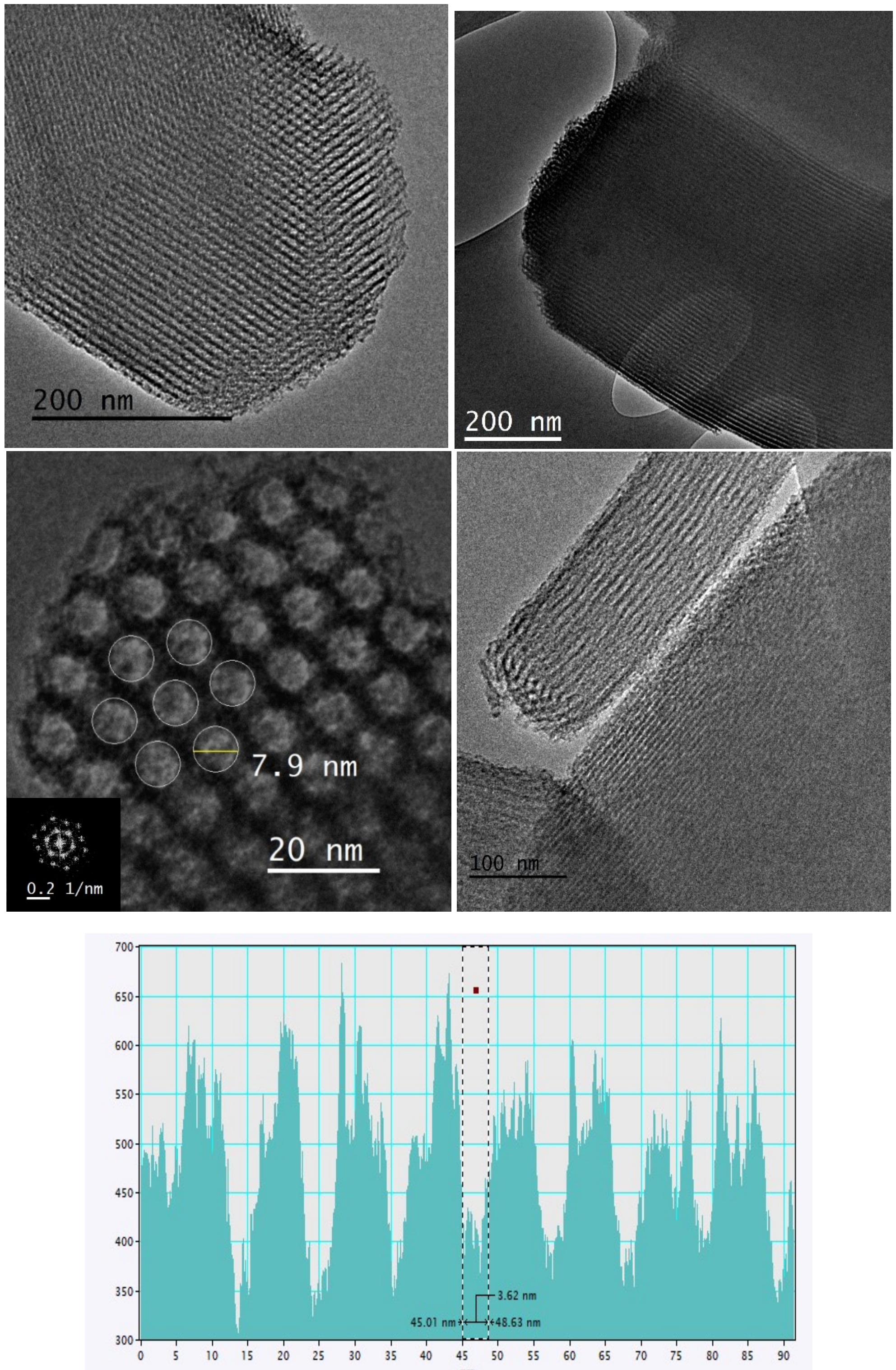

Figure S10. TEM micrographs of pristine calcinated SBA-15 where it showed a ca. 7.9 nm of pore dimeter and 3.6 nm of walls width.

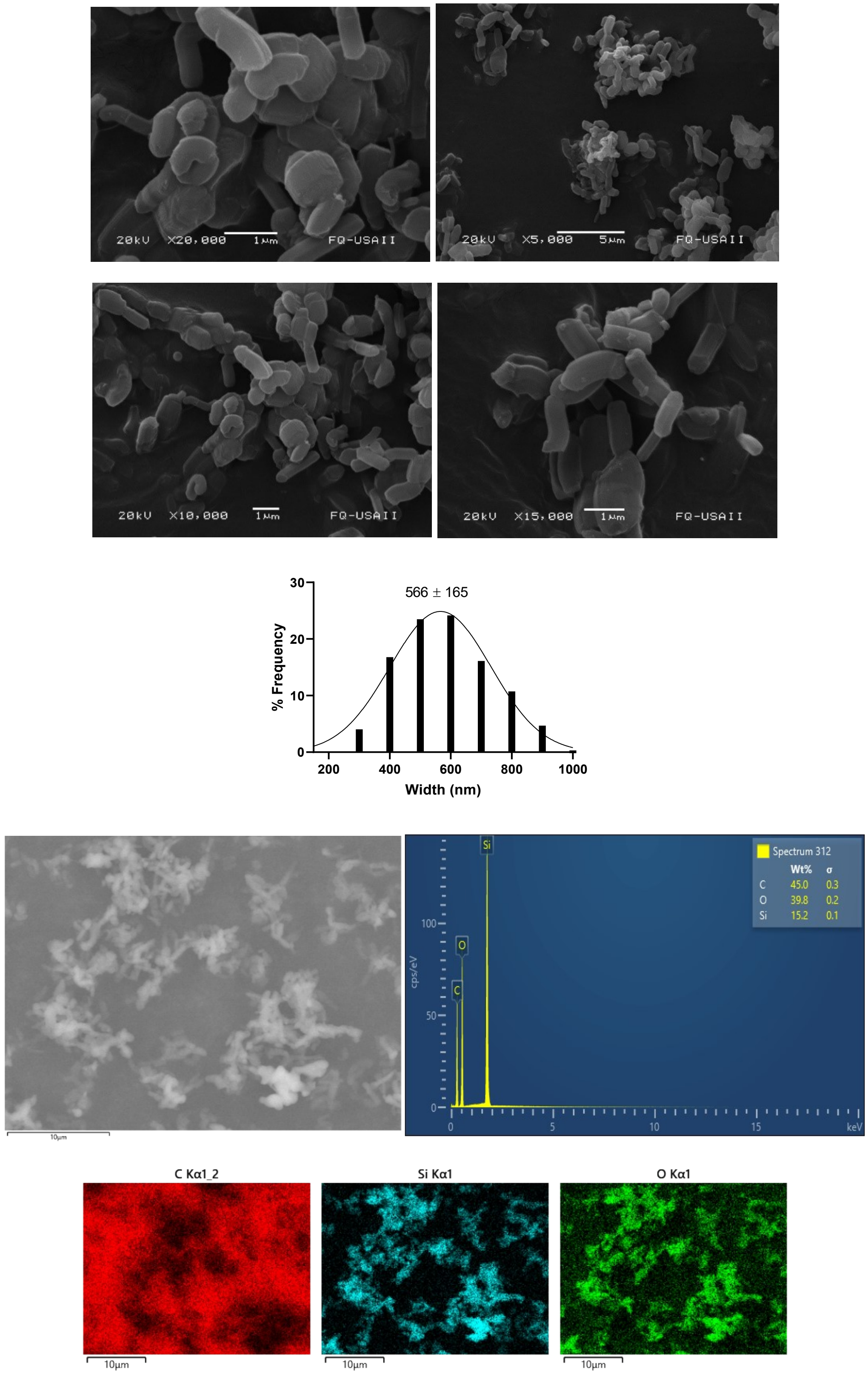

Figure S11. SEM micrographs of pristine calcinated SBA-15 with particles size distribution (566 ±165) with EDX and element mapping.

H. TEM micrographs with EDX analysis of RhNPs@MMS

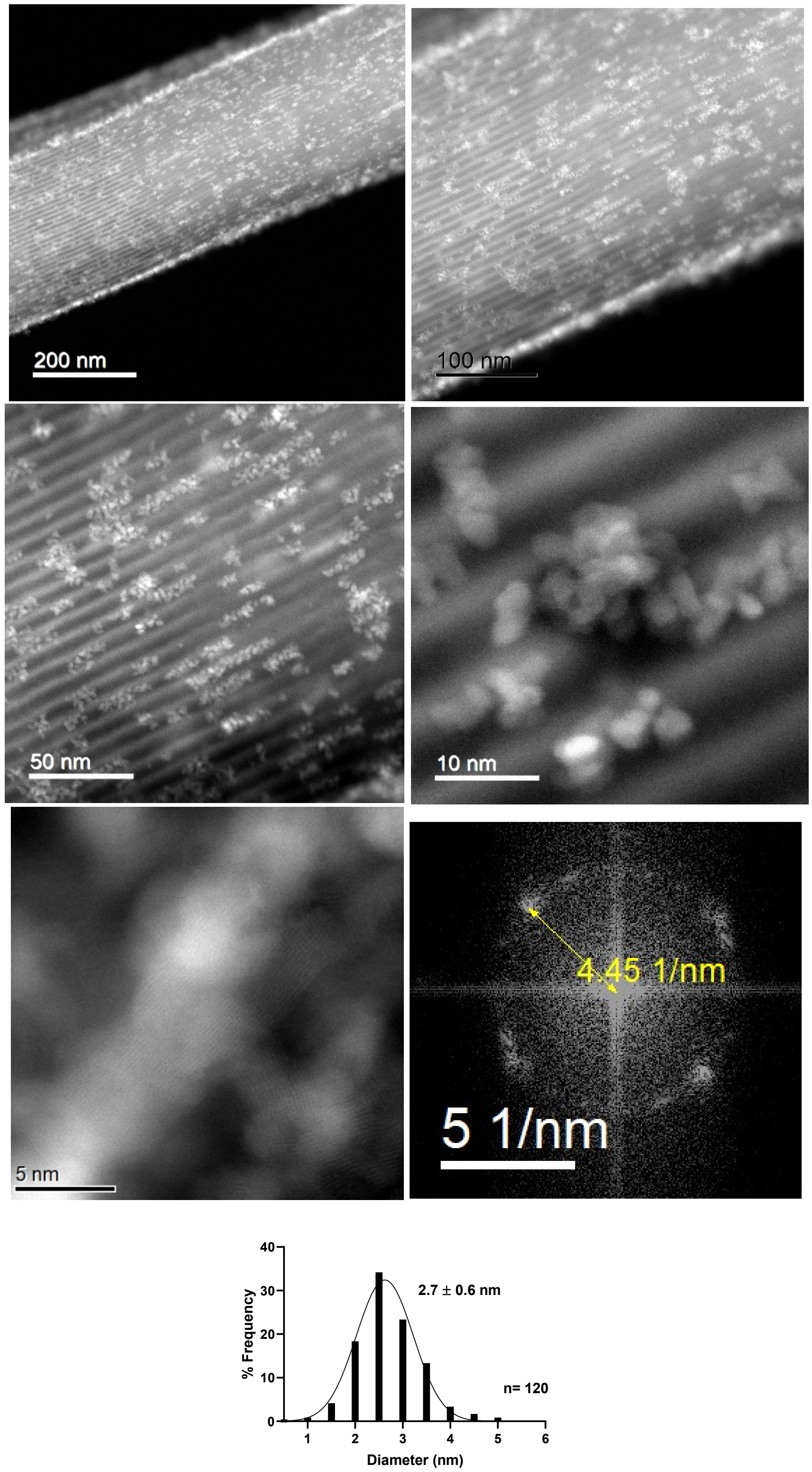

Figure S12. HAADF-STEM images of RhNPs@SBA-15-Imz[NTf_2] with FFT. Mean diameter: 2.7 ± 0.6 nm.

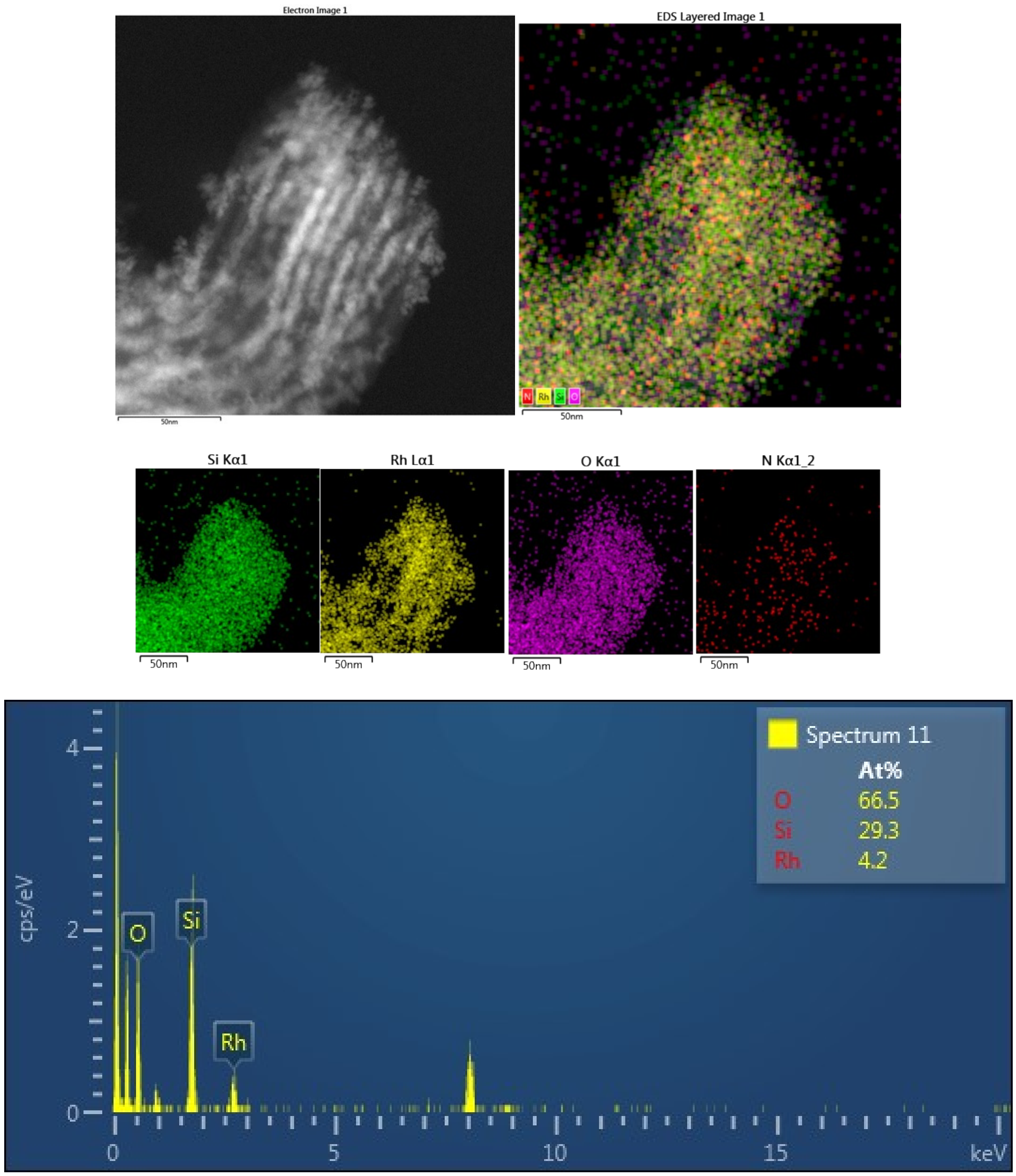

Element	Line Type	k Factor	k Factor type	Absorption Correction	Wt%	Wt% Sigma	Atomic %
N	K series	3.515	Theoretical	1.00	0.00	0.00	0.00
O	K series	2.020	Theoretical	1.00	44.48	0.51	63.46
Si	K series	1.000	Theoretical	1.00	38.61	0.45	31.38
Cl	K series	1.026	Theoretical	1.00	3.33	0.20	2.14
Rh	L series	1.814	Theoretical	1.00	13.58	0.60	3.01
Total					100.00		100.00

Figure S13. Element mapping and EDX quantification of RhNPs@SBA-15-Imz[NTf_2]

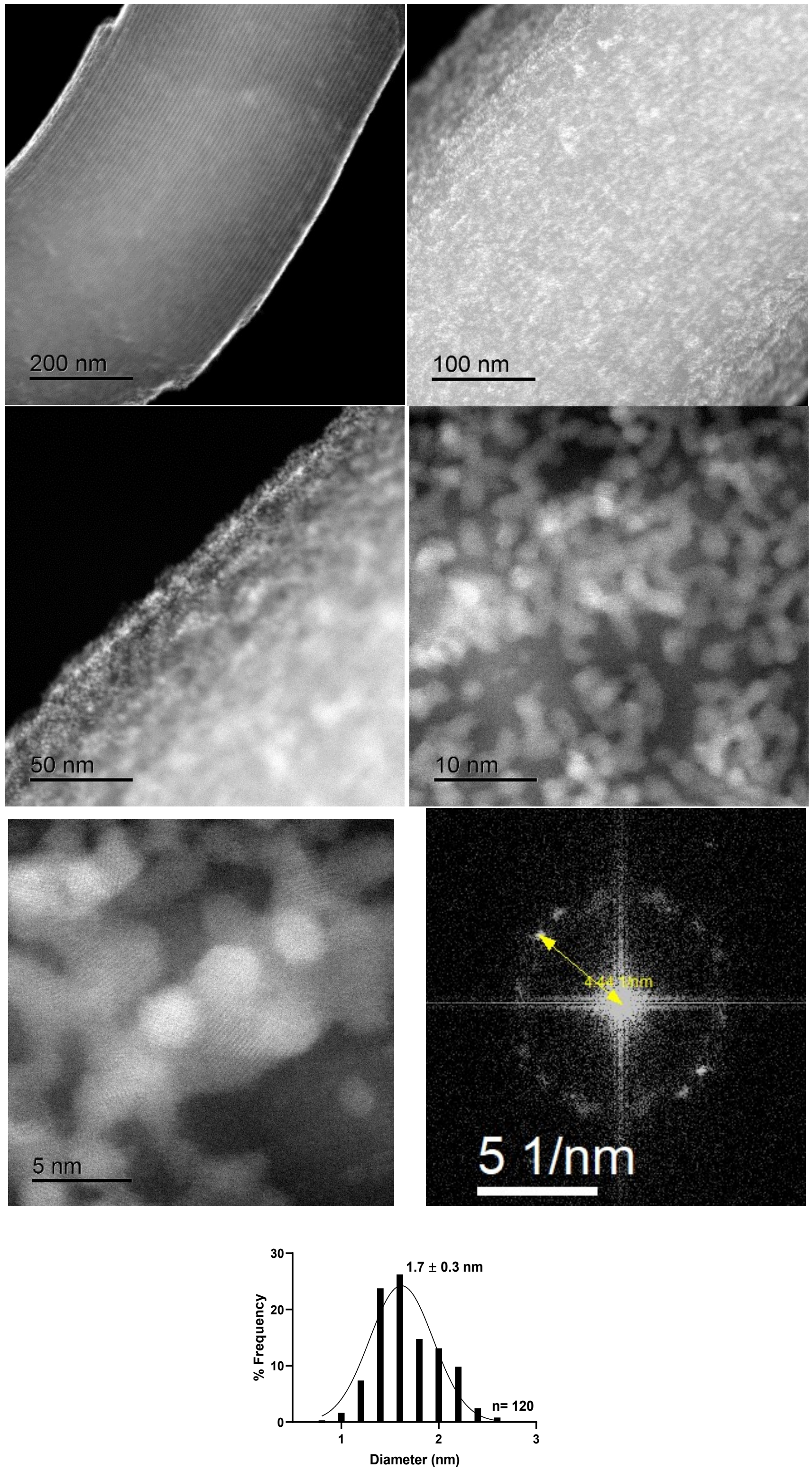

Figure S14. HAADF-STEM images of RhNPs@SBA-15NIC with FFT. Mean diameter: 1.7 ± 0.3 nm.

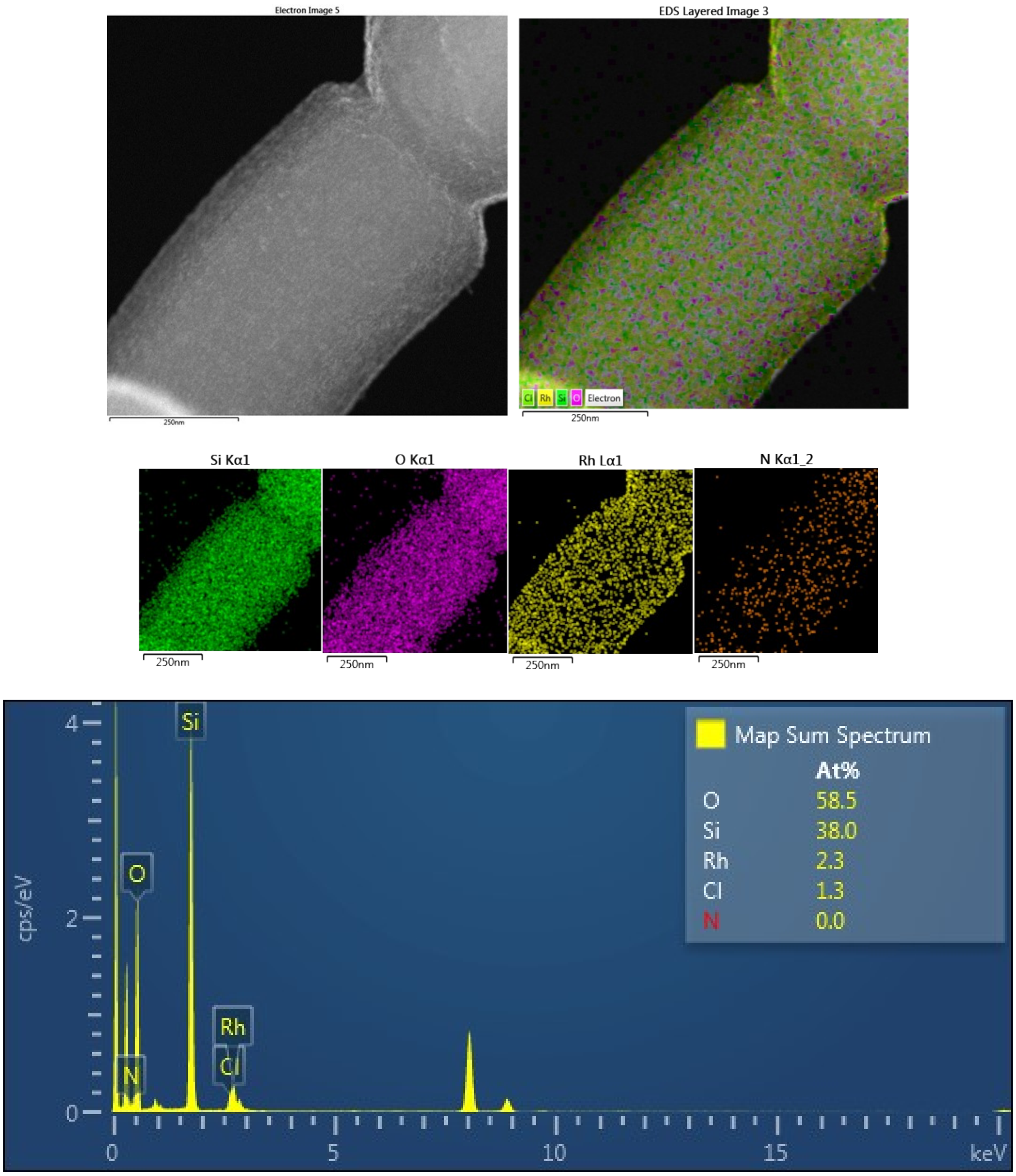

Element	Line Type	k Factor	k Factor type	Absorption Correction	Wt%	Wt% Sigma	Atomic %
N	K series	3.515	Theoretical	1.00	0.00	0.00	0.00
O	K series	2.020	Theoretical	1.00	40.98	0.33	58.45
Si	K series	1.000	Theoretical	1.00	46.75	0.32	37.98
Cl	K series	1.026	Theoretical	1.00	2.00	0.11	1.29
Rh	L series	1.814	Theoretical	1.00	10.27	0.36	2.28
Total					100.00		100.00

Figure S15. Element mapping and EDX quantification of RhNPs@SBA-15-NIC

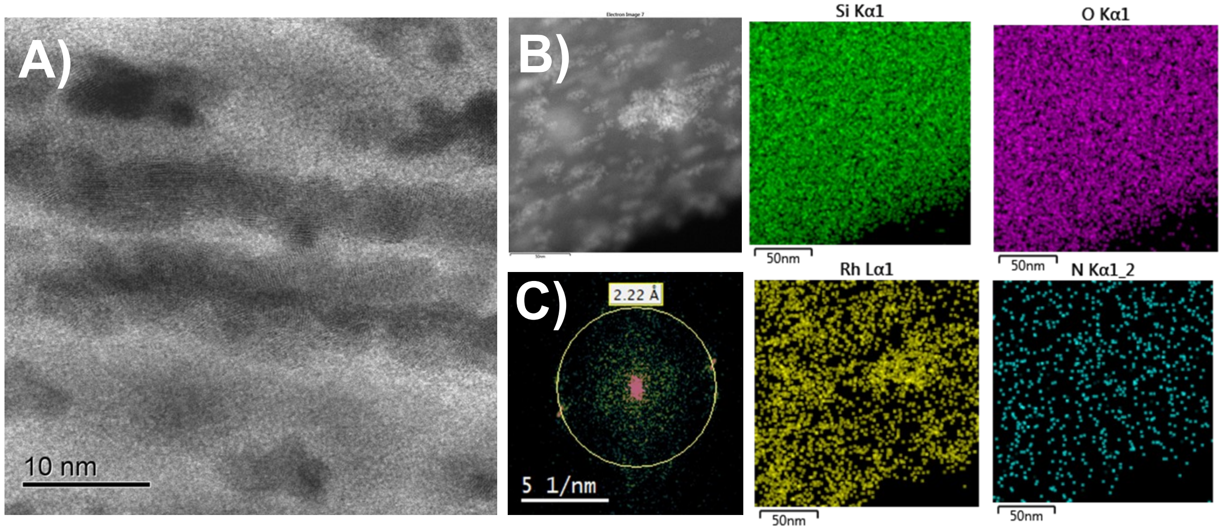

Figure S16. STEM image of RhNPs in spent catalyst (A) with EDX elemental mapping (B) and FFT of RhNPs (C).

I. XPS spectra of RhNPs@MMS

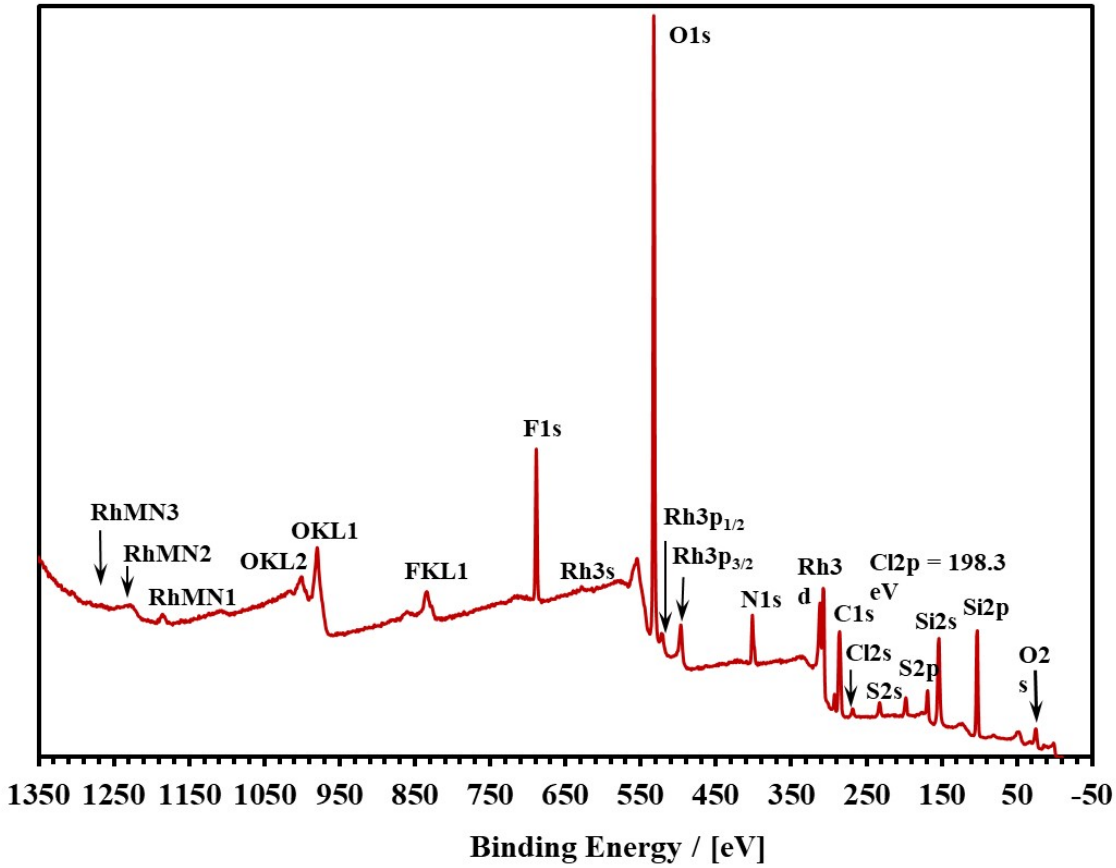

Figure S17. XPS survey of RhNPs@SBA-15Imz[NTf2]

Table S3 Element distribution on surface of RhNPs@SBA-15Imz[NTf2] by XPS

Name	Peak BE	Atomic %	Wt. %
O1s	532.95	40.07	31.8
Rh3d	**307.93**	**2.24**	**11.4**
F1s	689.03	8.26	7.8
Si2p	103.38	18.56	25.9
C1s	286.13	20.86	12.4
N1s	401.82	6.17	4.3
S2p	169.23	2.59	4.1
Cl2p	198.3	1.25	2.2

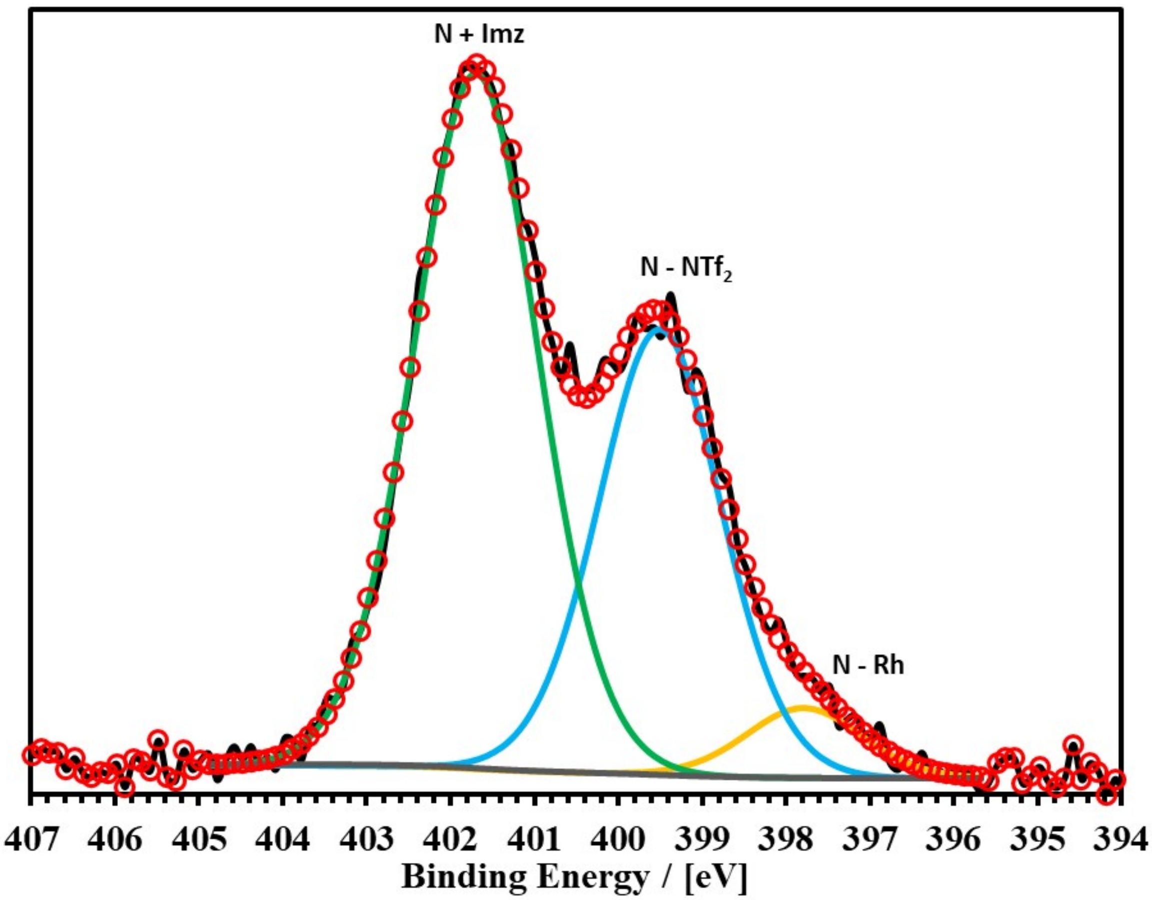

Figure S18. High resolution -XPS of N 1s in RhNPs@SBA-15Imz[NTf2]

Table S4 Nitrogen species distribution on surface of RhNPs@SBA-15Imz[NTf2] by XPS

Name	Peak BE	Atomic %
N*-Rh	397.83	5.42
N^- (NTf_2)	399.09	36.65
N^+ (Imz)	401.28	57.93

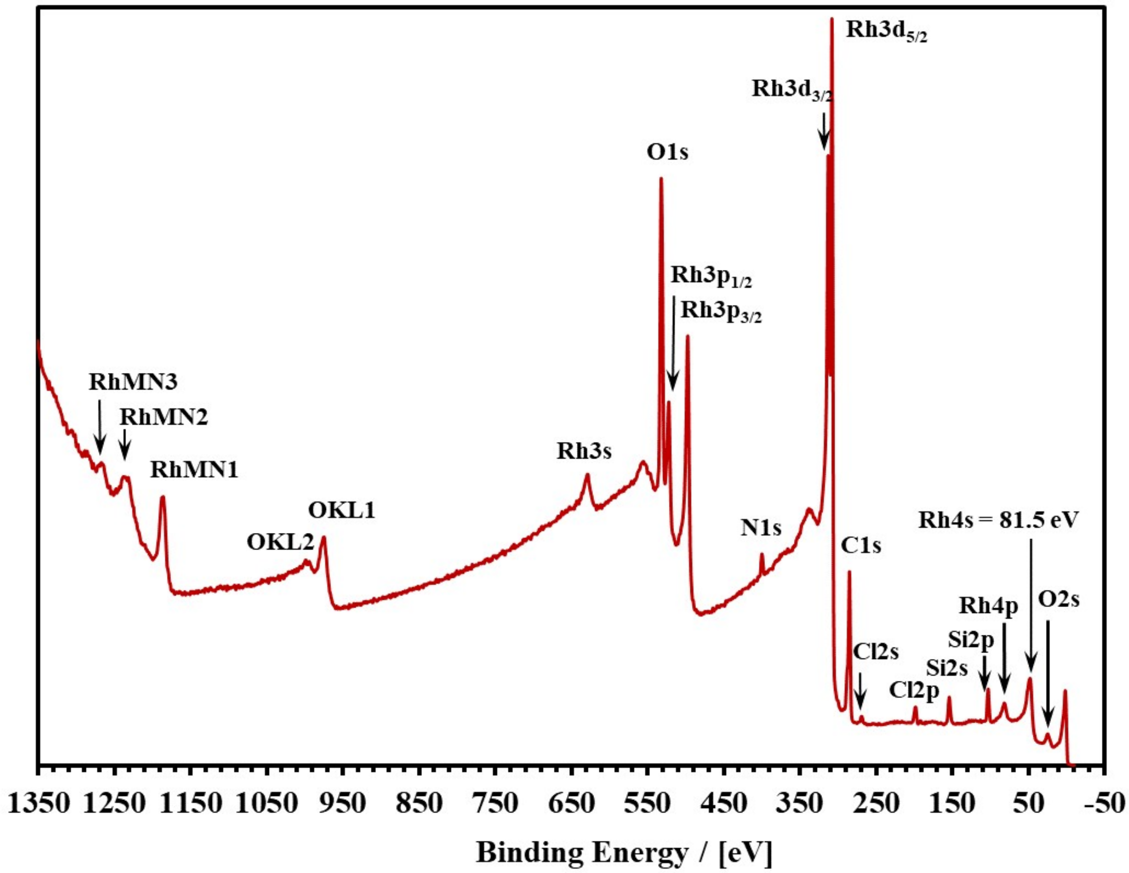

Figure S19. XPS survey of RhNPs@SBA-15NIC

Table S5 Element distribution on surface of RhNPs@SBA-15NIC by XPS

Name	Peak BE	Atomic %	Wt. %
Rh3d	308.14	14.99	53.78
O1s	531.81	36.12	20.15
C1s	285.2	36.18	15.15
Si2p	103.17	6.87	6.73
N1s	399.91	4.03	1.97
Cl2p	198.56	1.81	2.24

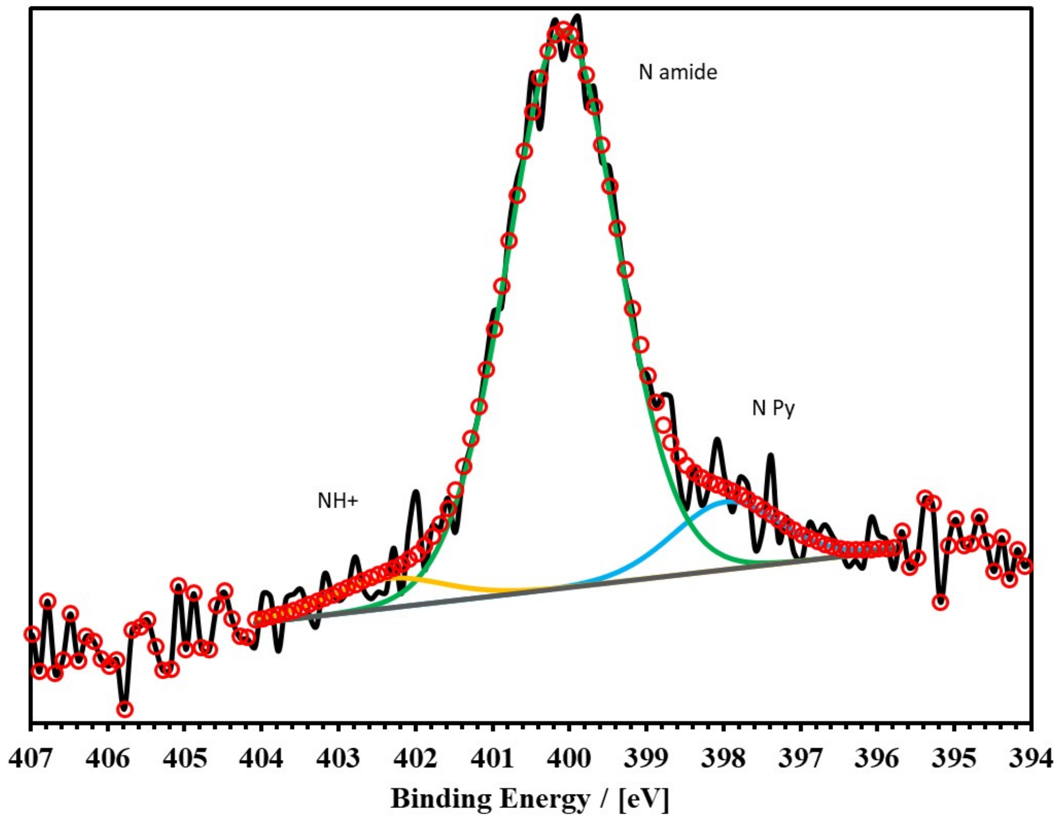

Figure S20. High resolution -XPS of N 1s in RhNPs@SBA-15NIC

Table S6 Nitrogen species distribution on surface of RhNPs@SBA-15NIC by XPS

Name	Peak BE	Atomic %
N Pyridine	397.96	10.1
N amide	400.09	85.21
NH +	402.39	4.69

J. Calculation of specific surface area and metal Dispersion.

For the calculation of the dispersion (D) of the RhNPs, we assume nanoparticles as spheres; let NS be the total number of metal atoms present on the surface and NT the total number of metal atoms (surface and bulk). The metal dispersion D is given by

D = NS/NT (eq. 1)

Taking in account the relationship between specific surface area (S_{sp}) and dispersion (D) is

$S_{sp} = a_m (N_A/M)D$ (eq. 2)

Where a_m is the surface area occupied by an atom (Rh) on a polycrystalline surface, N_A is Avogadro's number (6.022×10^{23} mol^{-1}) and M is the atomic mass of the metal.

And the definition of v_m (the volume occupied by an atom (Rh) in the bulk of metal) given by:

$v_m = M/\rho NA$ (eq. 3)

where ρ the mass density

It possible to rewrite the D in terms of a_m, v_m and d_{NP}.[1,2] and rewrites as follows:

$D = [6(v_m/a_m)]/d_{NP}$ (eq. 4)

Where d_{Np} is the mean diameter of nanoparticles.

For Rh (FCC) a_m = 7.58 $Å^2$, v_m = 13.78 $Å^3$, ρ= 12.4 g cm^{-3},

D(RhNPs@SBA-15Imz[NTf$_2$]) = [6*(13.78 $Å^3$/7.58 $Å^2$)]/ **27** Å = ***0.404 (40.4 %)***

S_{Sp} (RhNPs@SBA-15Imz[NTf$_2$])= $7.58 \times 10^{-20} m^2$ (N_A/102.905)=443.6*D= ***179 m^2g^{-1}***

D(RhNPs@SBA-15NIC)= [6*(13.78 $Å^3$/7.58 $Å^2$)]/ **17** Å = ***0.642 (64.2 %)***

S_{Sp} (RhNPs@SBA-15Imz[NTf$_2$])= $7.58 \times 10^{-20} m^2$ (N_A /102.905 g mol^{-1})=443.6*D= ***285 m^2g^{-1}***

K. Selected catalytic Reactions.

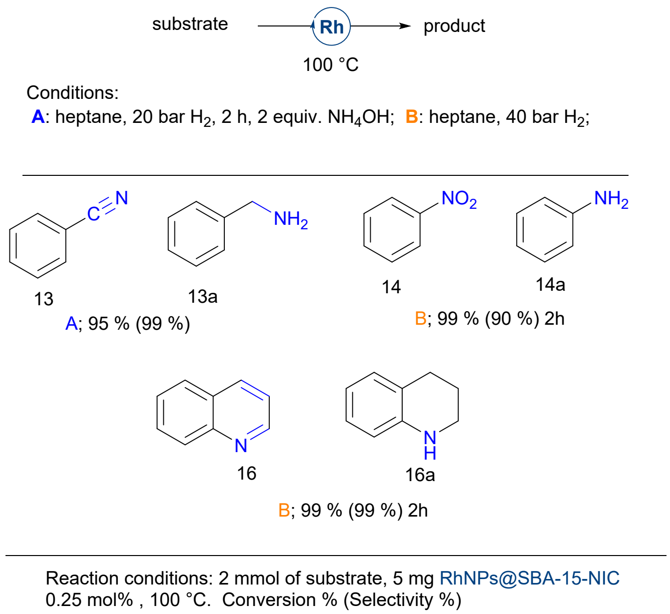

Figure S21. RhNPs@SBA-15NIC hydrogenation of different functional groups.

Table S7. Rh-catalyzed hydrogenation of Levulinic Acid.

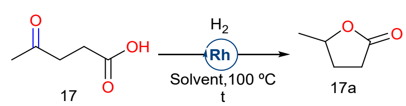

Entry	Catalyst	Solvent	Time (h)	H_2 (bar)	Conv.%[a]	Yield 17a%[a]	TON[b]
1	RhNPs@SBA-15-NIC	Dioxane	2h	5	<1	n.d.	n.d.
2				40	5	n.d.	n.d.
3		2-MeTHF			5	n.d.	n.d.
4		Heptane			<1	n.d.	n.d.
5		Neat	4		**15**	**12**	**96**
6	RhNPs@SBA-15-Imz[NTf$_2$]	Dioxane	2h	5	<1	n.d.	n.d.
7				40	18	9	72
8		2-MeTHF			7	n.d.	n.d.
9		Heptane			<1	n.d.	n.d.
10		Neat	4		**42**	**42**	**336**

Reaction conditions: Levulinic acid (203 µL, 2 mmol), 2 mL of solvent, 5 mg of catalyst, 100 °C.

Table S8. Rh-catalyzed hydrogenation of Furfural.

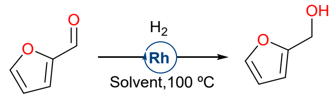

<table>
<tr><th>Entry</th><th>Catalyst</th><th>Solvent</th><th>Time (h)</th><th>H_2 (bar)</th><th>Conv.%[a]</th><th>Yield 17a%[a]</th><th>TON[b]</th></tr>
<tr><td>1</td><td rowspan="8">RhNPs@SBA-15-Imz[NTf$_2$]</td><td rowspan="2">Heptane</td><td rowspan="4">4</td><td>5</td><td><1</td><td>n.d.</td><td>n.d.</td></tr>
<tr><td>2</td><td>40</td><td><1</td><td>n.d.</td><td>n.d.</td></tr>
<tr><td>3</td><td rowspan="2">EtOH</td><td>5</td><td>25</td><td>77</td><td>154</td></tr>
<tr><td>4</td><td>40</td><td>30</td><td>57</td><td>137</td></tr>
<tr><td>5</td><td>MeOH</td><td>2</td><td rowspan="8">40</td><td>30</td><td>65</td><td>156</td></tr>
<tr><td>6</td><td>Dioxane</td><td rowspan="2">4</td><td>19</td><td>44</td><td>67</td></tr>
<tr><td>7</td><td rowspan="2">Neat</td><td>32</td><td>78</td><td>200</td></tr>
<tr><td>8</td><td>6</td><td>47</td><td>62</td><td>233</td></tr>
<tr><td>9</td><td rowspan="4">RhNPs@SBA-15-NIC</td><td>Heptane</td><td>4</td><td><1</td><td>n.d.</td><td>n.d.</td></tr>
<tr><td>10</td><td>MeOH</td><td>2</td><td>32</td><td>60</td><td>154</td></tr>
<tr><td>11</td><td>Dioxane</td><td rowspan="2">4</td><td>27</td><td>16</td><td>37</td></tr>
<tr><td>12</td><td>Neat</td><td>44</td><td>56</td><td>197</td></tr>
</table>

Reaction conditions: Furfural (166 µL, 2 mmol), 2 mL of solvent, 5 mg of catalyst, 100 °C.

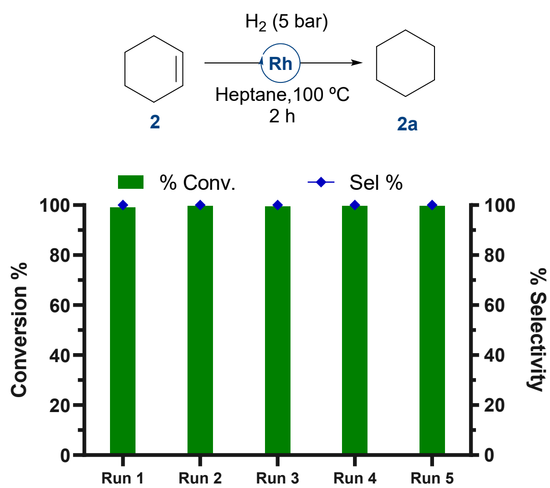

Scheme S1. Recycling experiments of RhNPs@SBA-15-Imz[NTf$_2$] on cyclohexene hydrogenation.

L. NMR Data of catalytic products

4-cyclohexylmorpholine: [3]

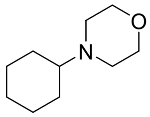

^{1}H NMR (600 MHz, $CDCl_3$) δ 3.79 – 3.71 (m, 4H), 2.67 – 2.55 (m, 4H), 2.29 – 2.17 (m, 1H), 1.96 – 1.74 (m, 4H), 1.37 – 1.13 (m, 6H).^{13}C NMR (151 MHz, $CDCl_3$) δ 66.90, 63.93, 49.44, 28.45, 26.09, 25.66.

Ethylbenzene:

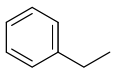

^{1}H NMR (600 MHz, $CDCl_3$) δ: 7.35 – 7.25 (m, 3H, Ar-H), 7.26 – 7.15 (m, 1H, Ar-H), 2.67 (q, *J* = 7.6 Hz, 2H, -CH_2-), 1.26 (t, *J* = 7.6 Hz, 3H, -CH_3).

Pinane: [4]

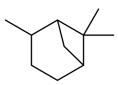

Mixture of Cis and Trans , ^{1}H NMR (600 MHz, $CDCl_3$) δ: 2.38 (q, *J* = 7.2 Hz, 2H), 2.20 (q, *J* = 8.1 Hz, 2H), 2.16 – 1.64 (m, 13H), 1.56 – 1.43 (m, 2H), 1.26 (d, *J* = 4.1 Hz, 9H), 1.08 (d, *J* = 12.0 Hz, 13H), 0.96 – 0.87 (m, 5H). ^{13}C NMR (151 MHz, $CDCl_3$) δ: 48.24, 47.79, 41.51, 41.03, 39.56, 38.90, 36.11, 35.57, 34.08, 29.48, 28.38, 26.91, 26.65, 24.72, 24.07, 23.97, 23.27, 23.14, 22.96, 21.65, 20.13.

5-propylbenzo[*d*][1,3]dioxole:

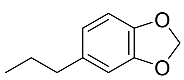

^{1}H NMR (600 MHz, , $CDCl_3$) δ: 6.83 – 6.69 (m, 2H), 6.69 – 6.61 (m, 1H), 5.93 (d, *J* = 1.1 Hz, 2H), 2.54 (t, *J* = 7.7 Hz, 2H), 1.67 – 1.60 (m, 2H), 0.97 (td, *J* = 7.3, 2.6 Hz, 3H). ^{13}C NMR (151 MHz, $CDCl_3$) δ: 147.59, 145.57, 136.65, 121.21, 109.00, 108.10, 100.77, 37.90, 24.93, 13.80.

1-methoxy-4-propylbenzene:

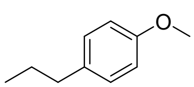

^{1}H NMR (600 MHz, $CDCl_3$) δ: 7.18 – 7.10 (m, 2H), 6.94 – 6.84 (m, 2H), 3.83 (s, 4H), 2.63 – 2.54 (m, 2H), 1.67 (h, *J* = 7.4 Hz, 2H), 0.99 (t, *J* = 7.4 Hz, 3H). ^{13}C NMR (151 MHz, $CDCl_3$) δ: 157.78, 134.91, 129.42, 113.75, 55.31, 37.27, 24.92, 13.89.

2-methoxy-4-propylphenol:

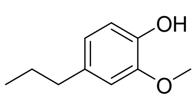

^{1}H NMR (600 MHz, $CDCl_3$) δ: 6.96 (d, *J* = 7.9 Hz, 1H), 6.82 – 6.74 (m, 2H), 5.91 (s, 1H), 3.90 (s, 3H), 2.65 – 2.60 (m, 2H), 1.73 (h, *J* = 7.4 Hz, 2H), 1.05 (t, *J* = 7.4 Hz, 3H). ^{13}C NMR (151 MHz, $CDCl_3$) δ: 146.38, 143.57, 134.58, 120.93, 114.23, 111.10, 55.70, 37.70, 24.82, 13.71.

2,6-dimethyloctane:

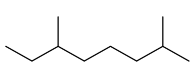

^{1}H NMR (600 MHz, $CDCl_3$) δ: 1.58 – 1.48 (m, 1H), 1.42 – 1.19 (m, 5H), 1.19 – 1.03 (m, 4H), 0.90 – 0.83 (m, 12H). ^{13}C NMR (151 MHz, $CDCl_3$) δ: 39.57, 37.07, 34.62, 29.71, 28.17, 25.02, 22.88, 22.79, 19.39, 11.58.

Stearic acid: [5]

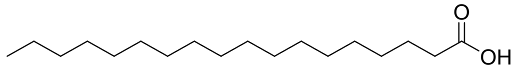

^{1}H NMR (600 MHz, $CDCl_3$) δ: 11.69 (s, 1H), 2.34 (t, *J* = 7.6 Hz, 2H), 1.63 (p, *J* = 7.5 Hz, 2H), 1.26 (s, 26H), 0.88 (t, *J* = 7.0 Hz, 3H). ^{13}C NMR (151 MHz, $CDCl_3$) δ: 180.62, 34.26, 32.09, 29.86, 29.85, 29.83, 29.80, 29.75, 29.59, 29.52, 29.40, 29.22, 24.83, 22.85, 14.26.

Squalane: [5]

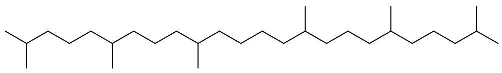

^{1}H NMR (600 MHz, $CDCl_3$) δ 1.65 – 1.51 (m, 3H), 1.52 – 1.24 (m, 25H), 1.25 – 1.06 (m, 12H), 0.99-0.82 (m, 24H). ^{13}C NMR (151 MHz, $CDCl_3$) δ 39.73, 37.82, 37.79, 37.77, 37.75, 37.66, 33.13, 33.10, 28.30, 27.80, 27.79, 25.17, 25.16, 24.82, 23.04, 22.94, 20.09, 20.06, 20.02, 20.00.

Benzylamine:

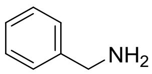

^{1}H NMR (600 MHz, , $CDCl_3$) δ: 7.31 – 7.17 (m, 5H), 3.77 (s, 2H), 1.39 (s, 2H). ^{13}C NMR (151 MHz, $CDCl_3$) δ: 143.07, 128.13, 126.70, 126.35, 46.10.

Aniline:

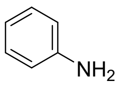

^{1}H NMR (600 MHz, $CDCl_3$) δ: 7.36 – 7.23 (m, 2H), 6.89 (t, *J* = 7.4 Hz, 1H), 6.82 – 6.68 (m, 2H), 3.68 (s, 2H). ^{13}C NMR (151 MHz, $CDCl_3$) δ: 146.42, 129.17, 118.31, 114.99.

Methylcyclohexane:[6]

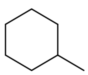

^{1}H NMR (600 MHz, $CDCl_3$) δ: 1.78 – 1.57 (m, 6H), 1.41 – 1.30 (m, 1H), 1.30 – 1.19 (m, 2H), 1.20 – 1.08 (m, 1H), 0.88 (d, *J* = 6.8 Hz, 3H). ^{13}C NMR (151 MHz, $CDCl_3$) δ: 35.66, 32.97, 26.67, 26.55, 23.05.

1,2,3,4-tetrahydroquinoline:[7]

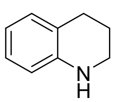

^{1}H NMR (600 MHz, $CDCl_3$) δ: 7.01 – 6.95 (m, 2H), 6.68 – 6.59 (m, 1H), 6.53 – 6.45 (m, 1H), 3.35 – 3.26 (m, 3H), 2.79 (t, *J* = 6.4 Hz, 2H), 2.00 – 1.92 (m, 2H). ^{13}C NMR (151 MHz, $CDCl_3$) δ: 144.88, 129.61, 126.82, 121.56, 117.05, 114.30, 42.08, 27.07, 22.28.

Gamma-valerolactone:[5]

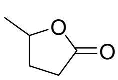

^{1}H NMR (600 MHz, $CDCl_3$) δ: 4.50 – 4.39 (m, 1H), 2.32 (dd, *J* = 10.2, 7.2 Hz, 2H), 2.23 – 2.10 (m, 1H), 1.69 – 1.58 (m, 1H), 1.20 – 1.16 (m, 3H). ^{13}C NMR (151 MHz, $CDCl_3$) δ: 176.89, 76.84, 29.19, 28.60, 20.53.

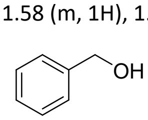

phenylmethanol ^{1}H NMR (600 MHz, $CDCl_3$) δ 7.51 – 7.29 (m, 5H), 4.59 (s, 2H), 4.18 (s, 1H). ^{13}C NMR (151 MHz, $CDCl_3$) δ: 140.79, 128.25, 127.23, 126.85, 64.44.

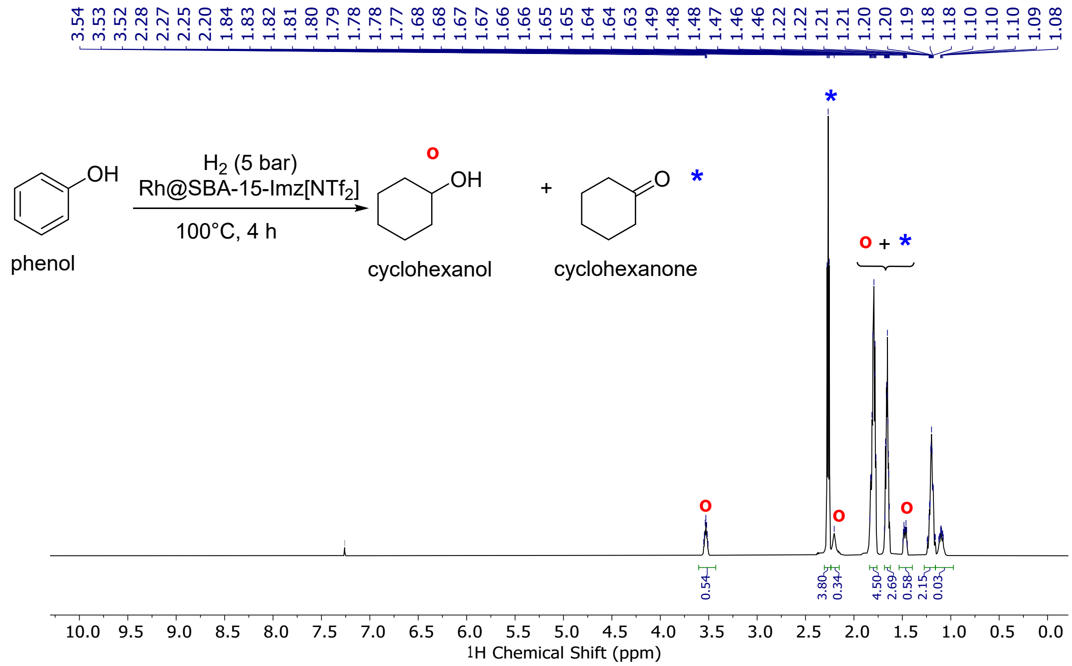
OH
phenol
H2 (5 bar)
Rh@SBA-15-Imz[NTf2]
100°C, 4 h
OH
cyclohexanol
+
O
cyclohexanone
1H Chemical Shift (ppm)

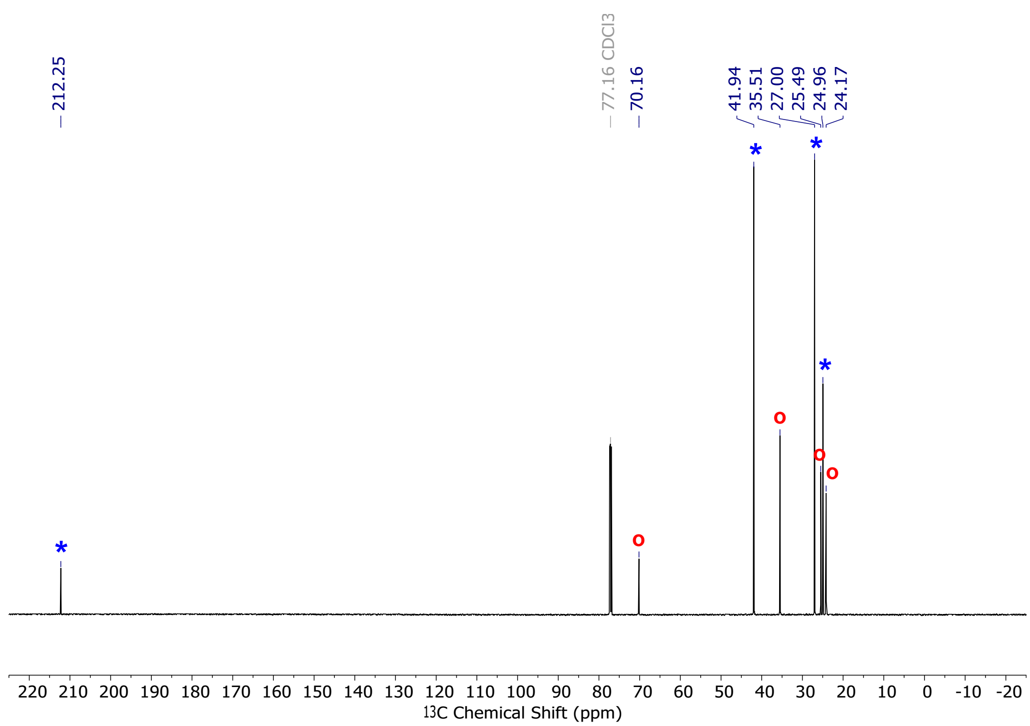
212.25
77.16 CDCl3
70.16
41.94
35.51
27.00
25.49
24.96
24.17
13C Chemical Shift (ppm)

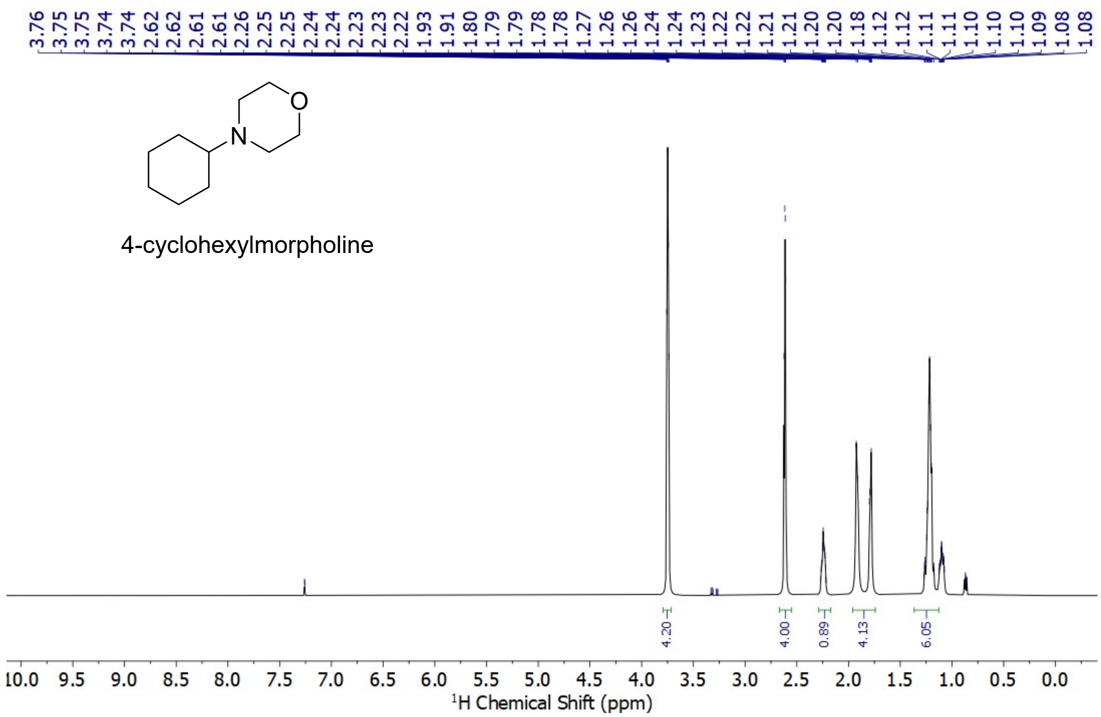

4-cyclohexylmorpholine

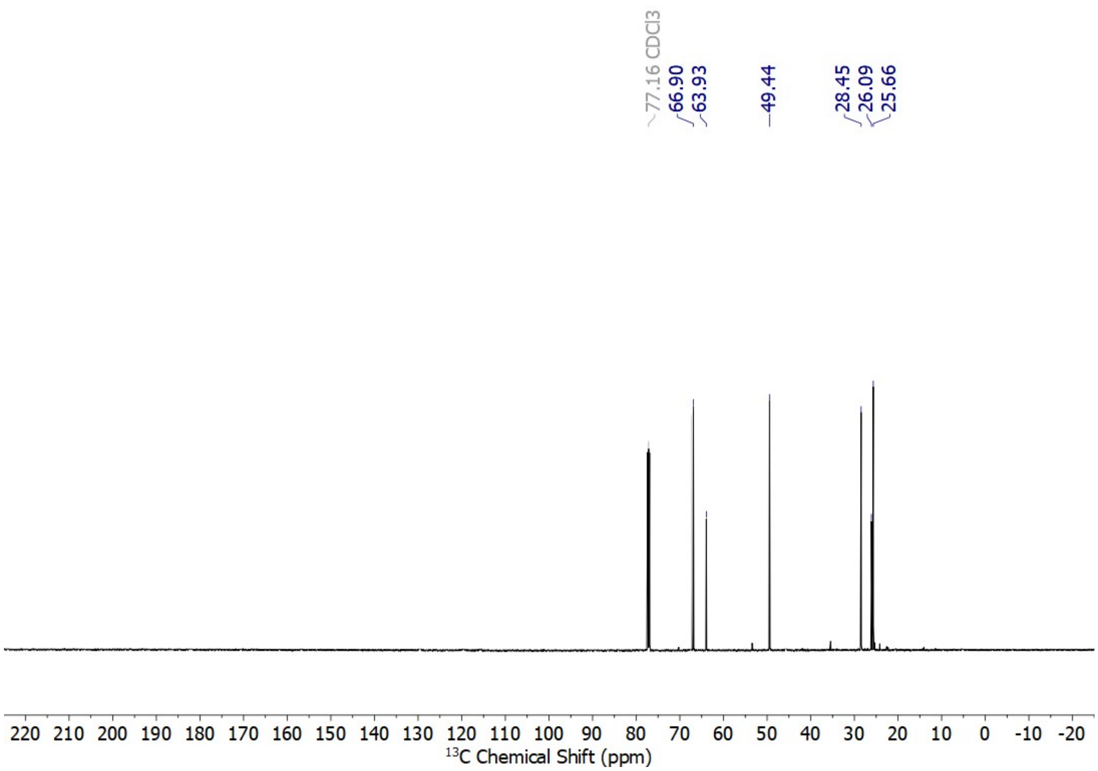

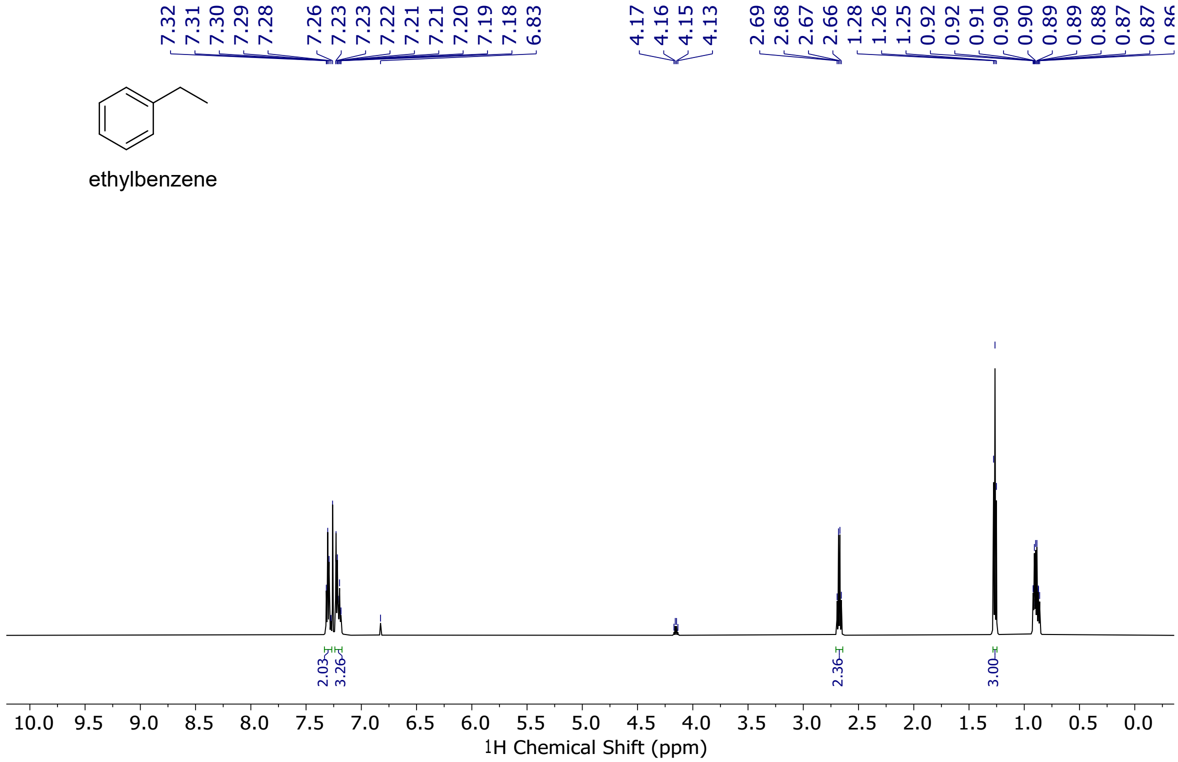
7.32
7.31
7.30
7.29
7.28
7.26
7.23
7.23
7.22
7.21
7.21
7.20
7.19
7.18
6.83
4.17
4.16
4.15
4.13
2.69
2.68
2.67
2.66
1.28
1.26
1.25
0.92
0.92
0.91
0.90
0.90
0.89
0.89
0.88
0.87
0.87
ethylbenzene
2.03
3.26
2.36
3.00
10.0 9.5 9.0 8.5 8.0 7.5 7.0 6.5 6.0 5.5 5.0 4.5 4.0 3.5 3.0 2.5 2.0 1.5 1.0 0.5 0.0
1H Chemical Shift (ppm)

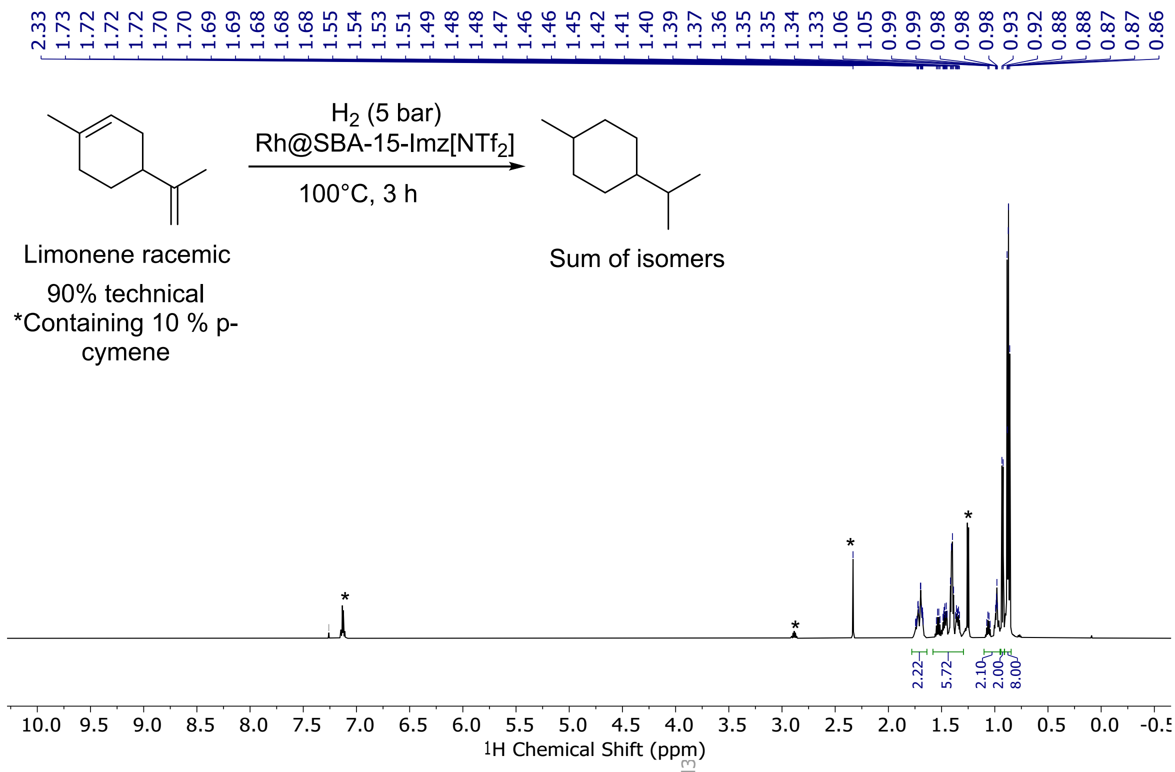
2.33 1.73 1.72 1.72 1.72 1.70 1.70 1.69 1.69 1.68 1.68 1.68 1.55 1.54 1.53 1.51 1.49 1.48 1.48 1.47 1.46 1.45 1.42 1.41 1.40 1.39 1.37 1.36 1.35 1.35 1.34 1.33 1.06 1.05 0.99 0.99 0.98 0.98 0.98 0.93 0.92 0.88 0.88 0.87 0.87 0.86
H2 (5 bar)
Rh@SBA-15-Imz[NTf2]
100°C, 3 h
Limonene racemic
90% technical
*Containing 10 % p-cymene
Sum of isomers
2.22
5.72
2.10
2.00
8.00
10.0 9.5 9.0 8.5 8.0 7.5 7.0 6.5 6.0 5.5 5.0 4.5 4.0 3.5 3.0 2.5 2.0 1.5 1.0 0.5 0.0 -0.5
1H Chemical Shift (ppm)

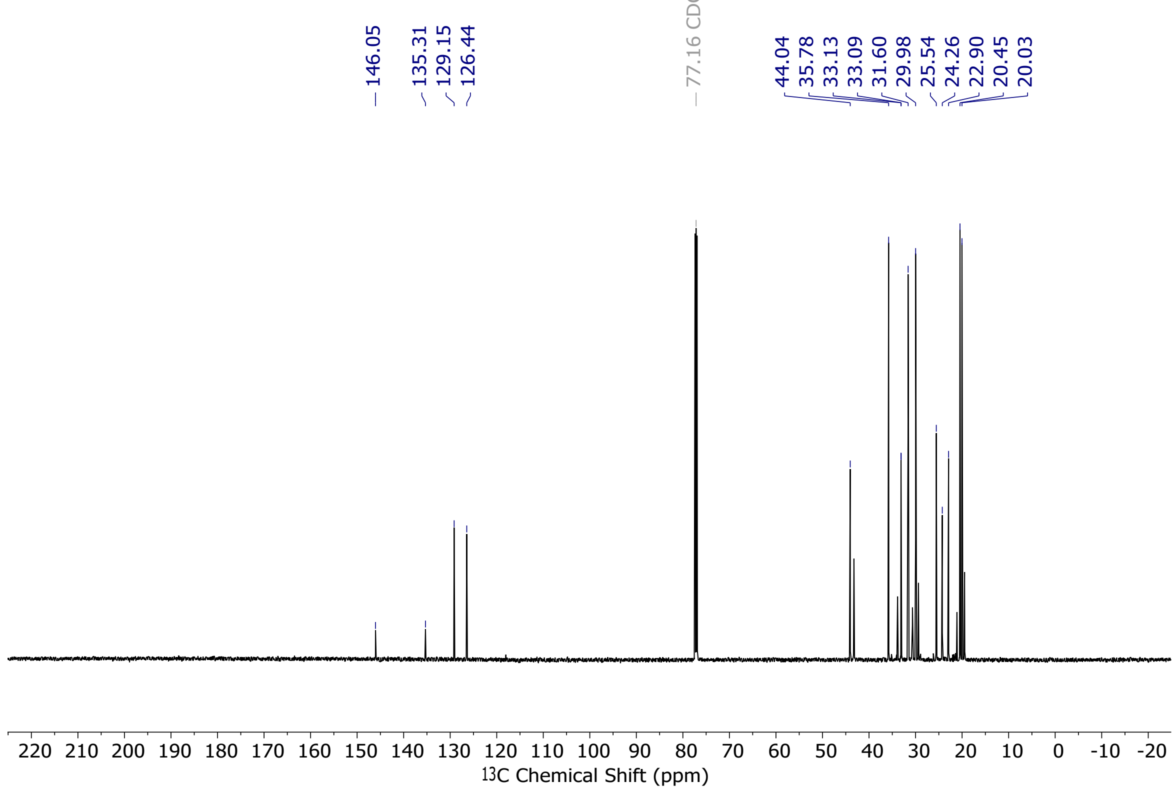
146.05
135.31 129.15 126.44
77.16 CDCl3
44.04 35.78 33.13 33.09 31.60 29.98 25.54 24.26 22.90 20.45 20.03
220 210 200 190 180 170 160 150 140 130 120 110 100 90 80 70 60 50 40 30 20 10 0 -10 -20
13C Chemical Shift (ppm)

Pinane
2,6,6-trimethylbicyclo[3.1.1]heptane

Mixture of cis and Trans
(1.8:1.0)

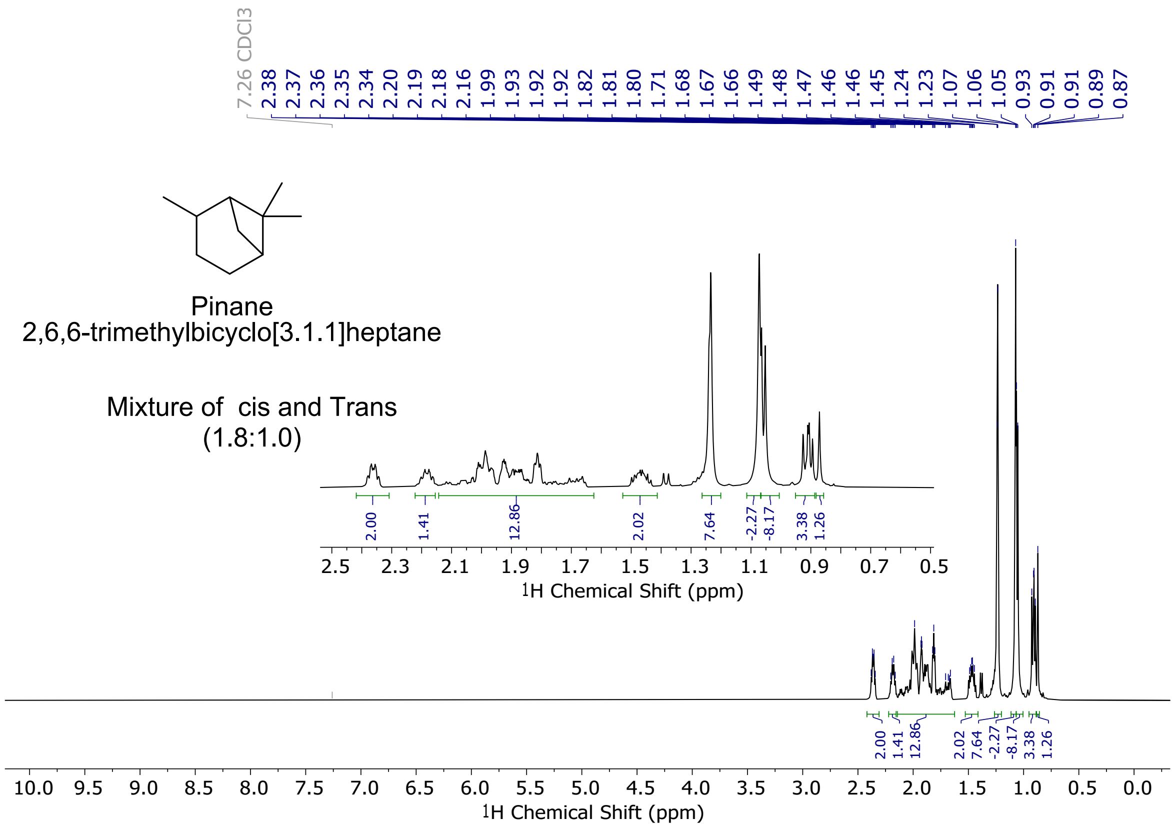

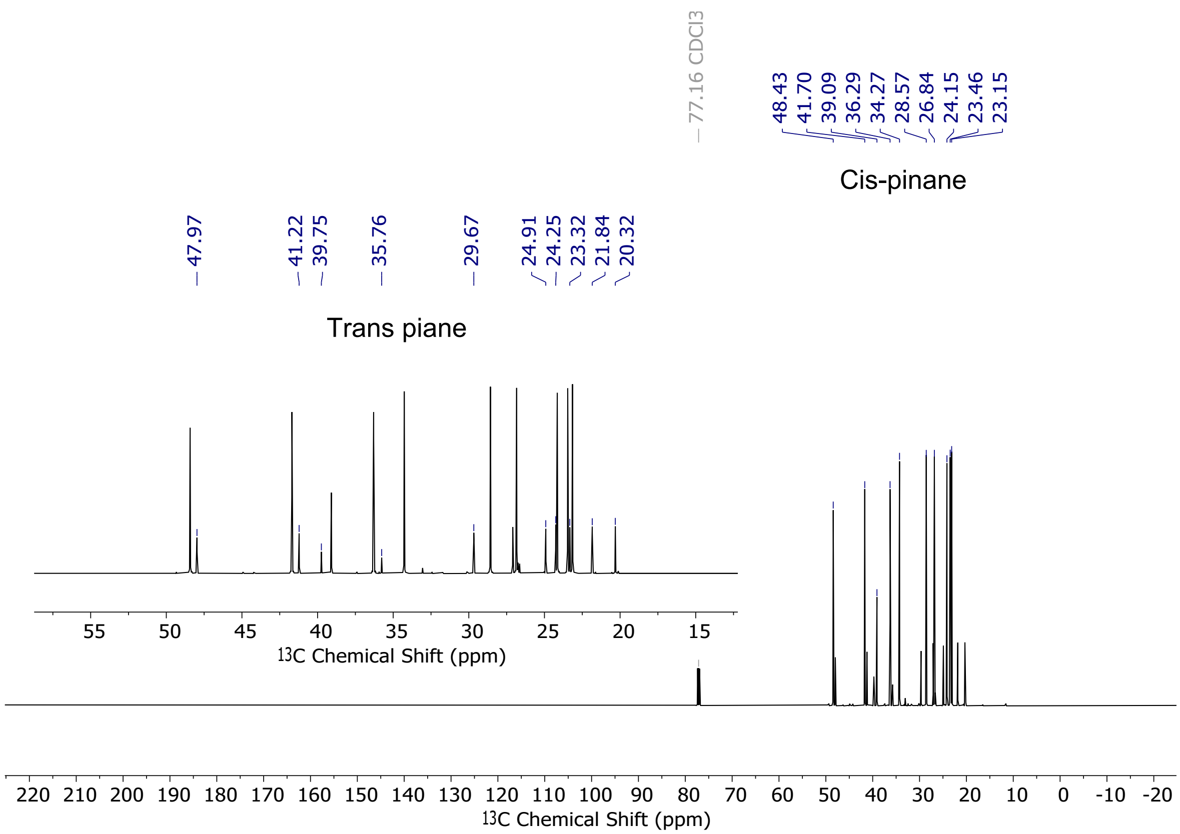

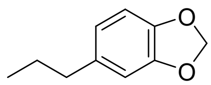

5-propylbenzo[*d*][1,3]dioxole

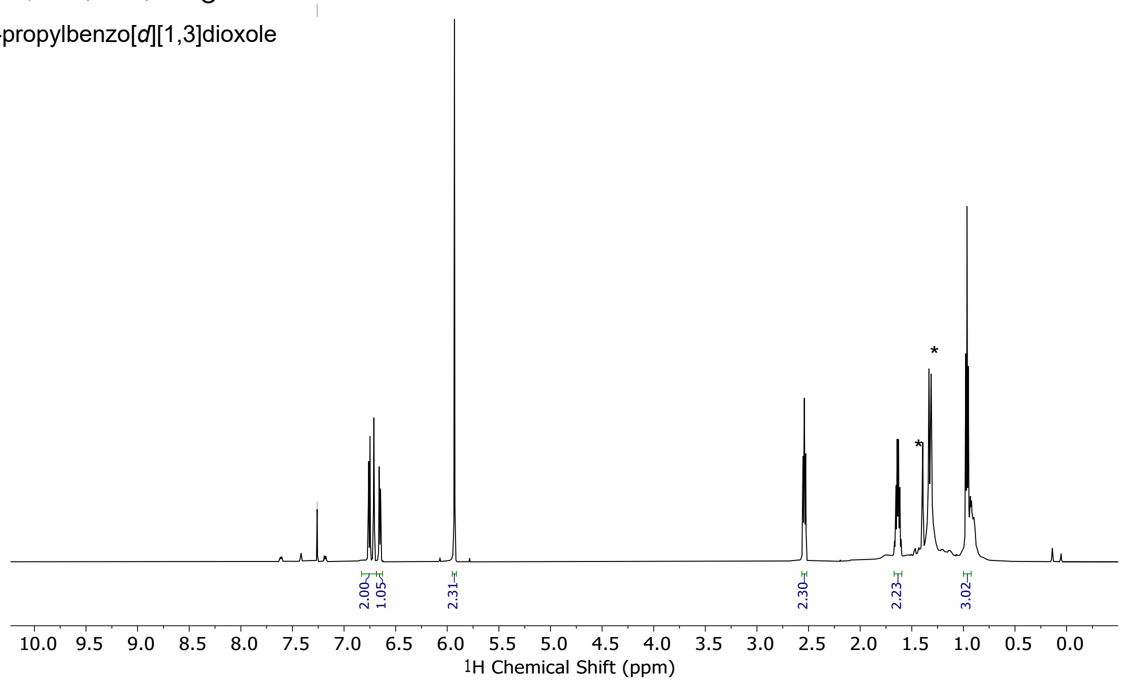

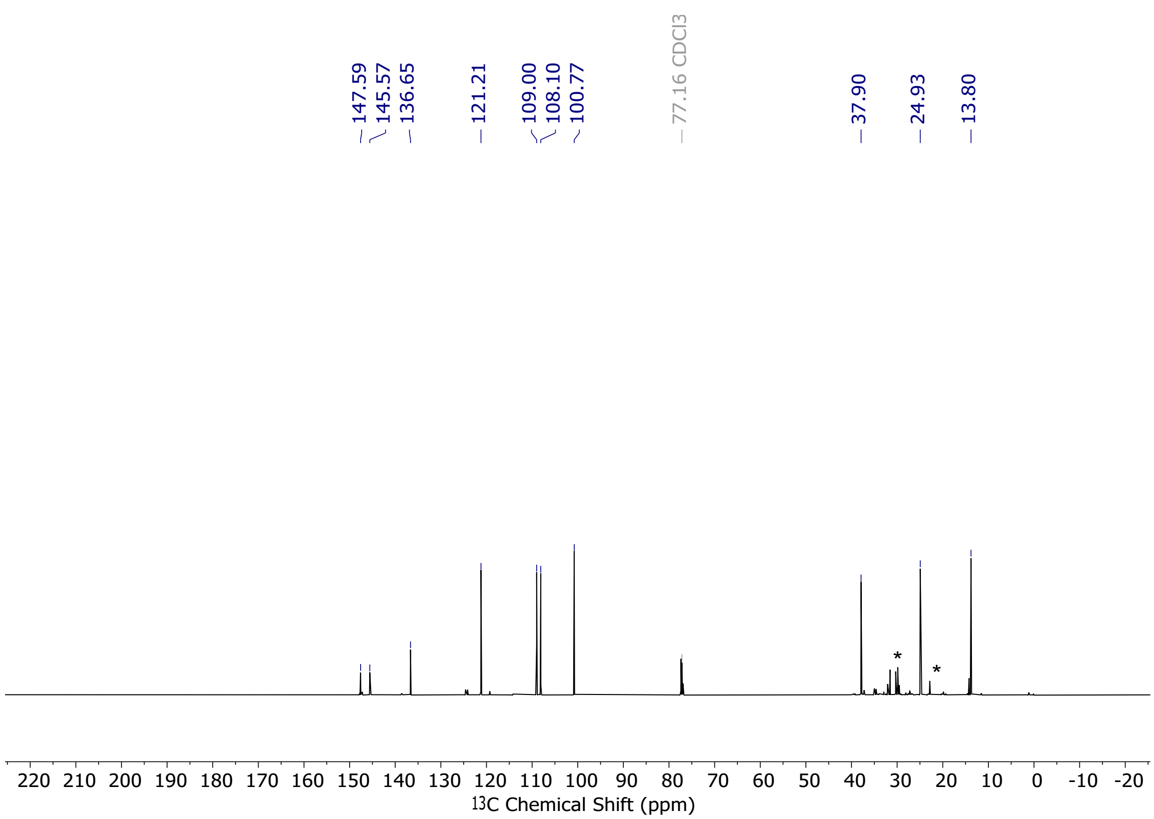

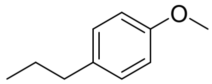

1-methoxy-4-propylbenzene

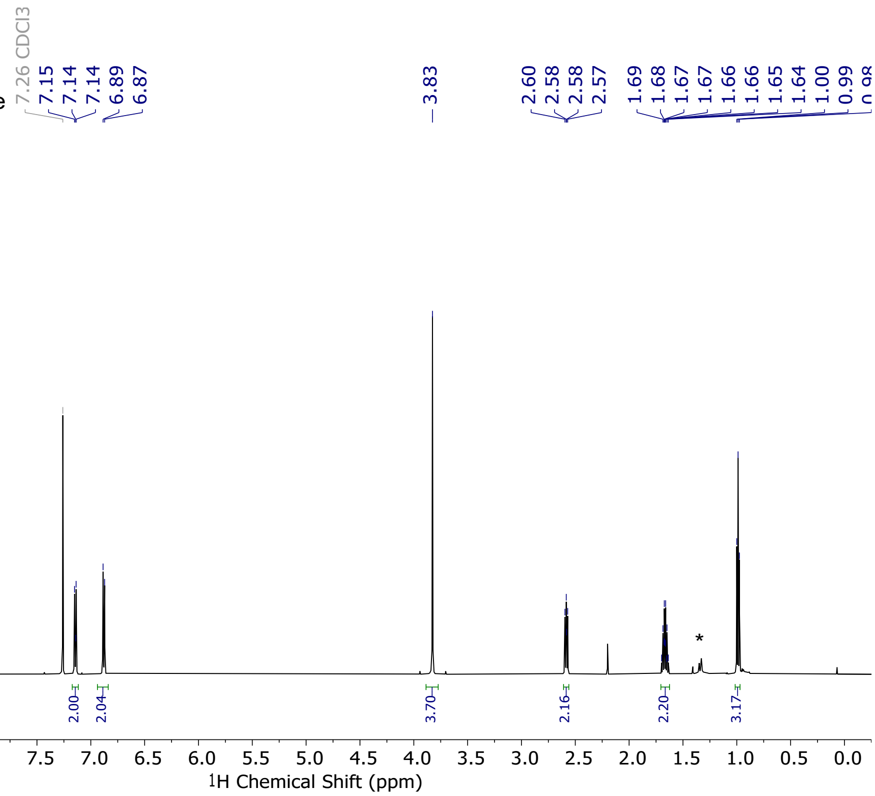

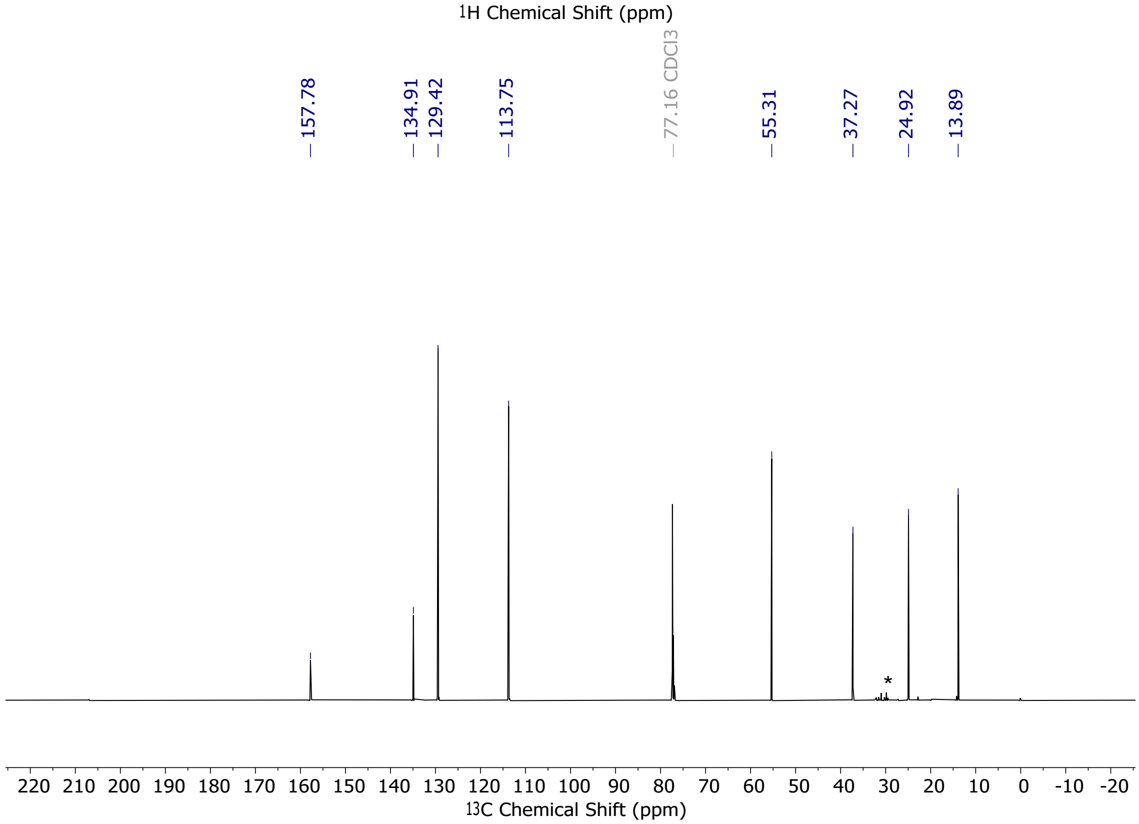

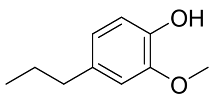

2-methoxy-4-propylphenol

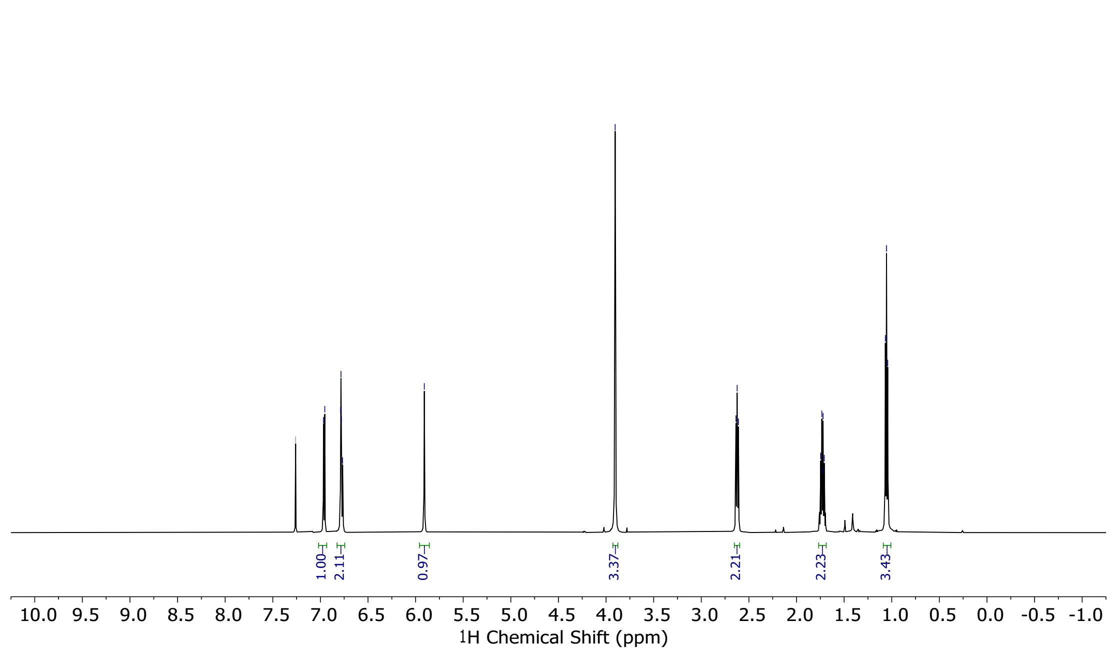

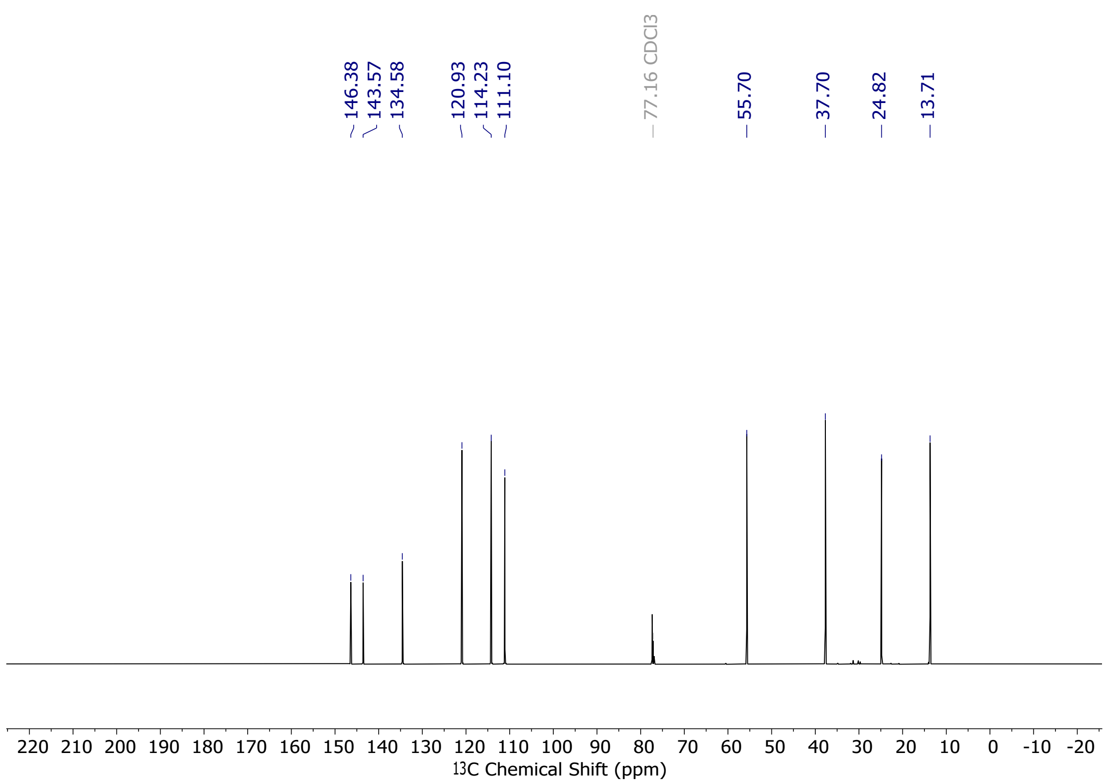

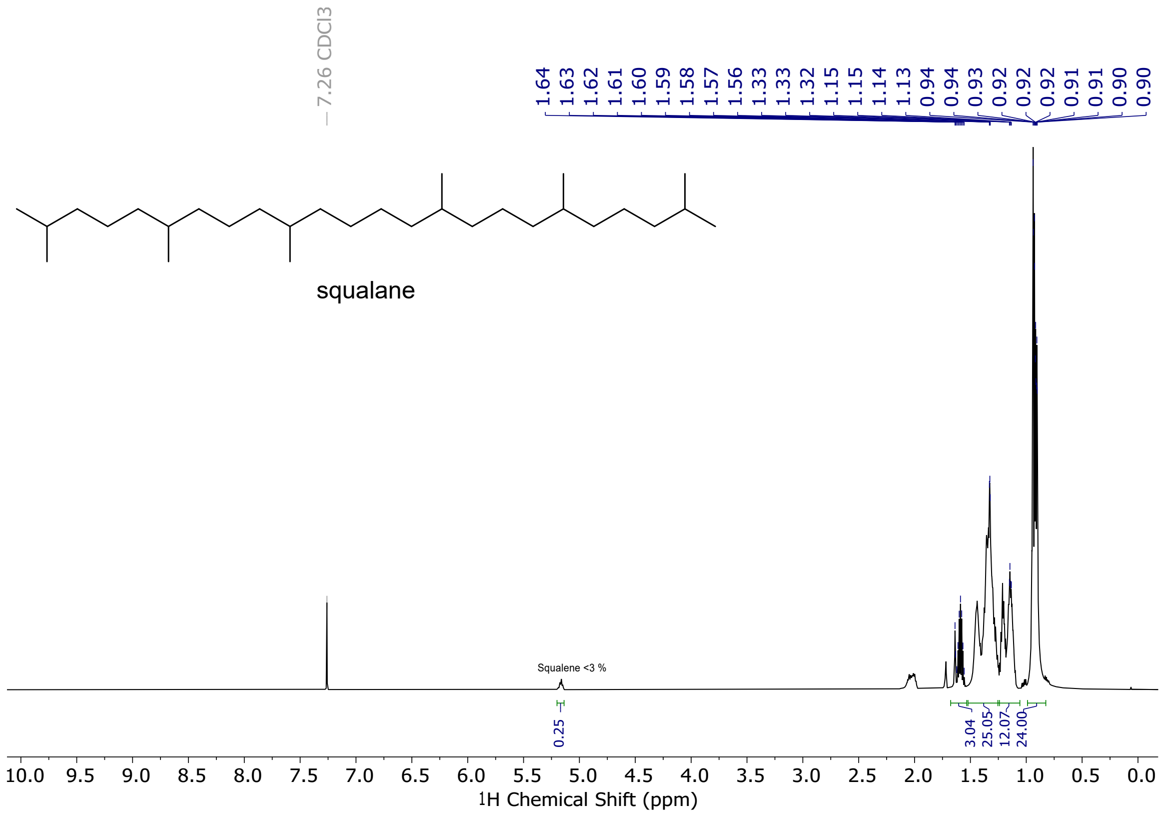
7.26 CDCl3
1.64 1.63 1.62 1.61 1.60 1.59 1.58 1.57 1.56 1.33 1.33 1.32 1.15 1.15 1.14 1.13 0.94 0.94 0.93 0.92 0.92 0.92 0.91 0.90 0.90
squalane
Squalene <3 %
0.25
3.04 25.05 12.07 24.00
10.0 9.5 9.0 8.5 8.0 7.5 7.0 6.5 6.0 5.5 5.0 4.5 4.0 3.5 3.0 2.5 2.0 1.5 1.0 0.5 0.0
1H Chemical Shift (ppm)

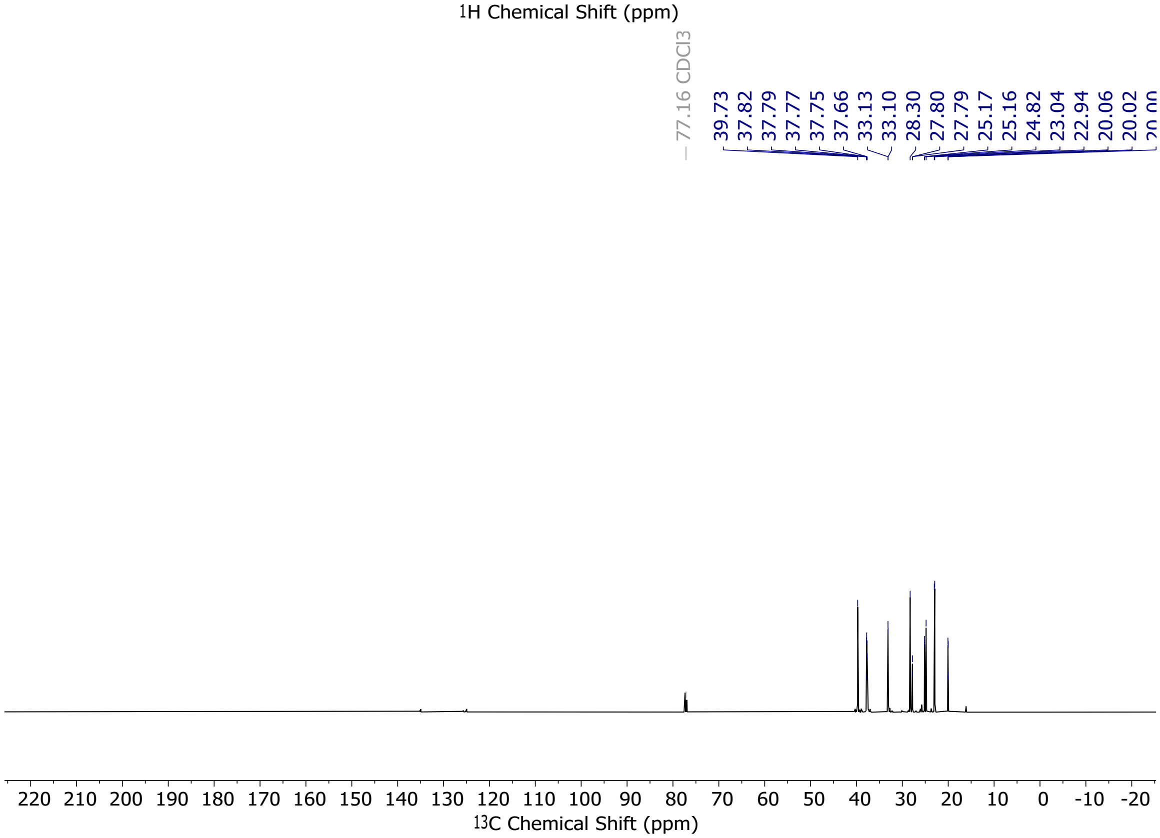
77.16 CDCl3
39.73 37.82 37.79 37.77 37.75 37.66 33.13 33.10 28.30 27.80 27.79 25.17 25.16 24.82 23.04 22.94 20.06 20.02
220 210 200 190 180 170 160 150 140 130 120 110 100 90 80 70 60 50 40 30 20 10 0 -10 -20
13C Chemical Shift (ppm)

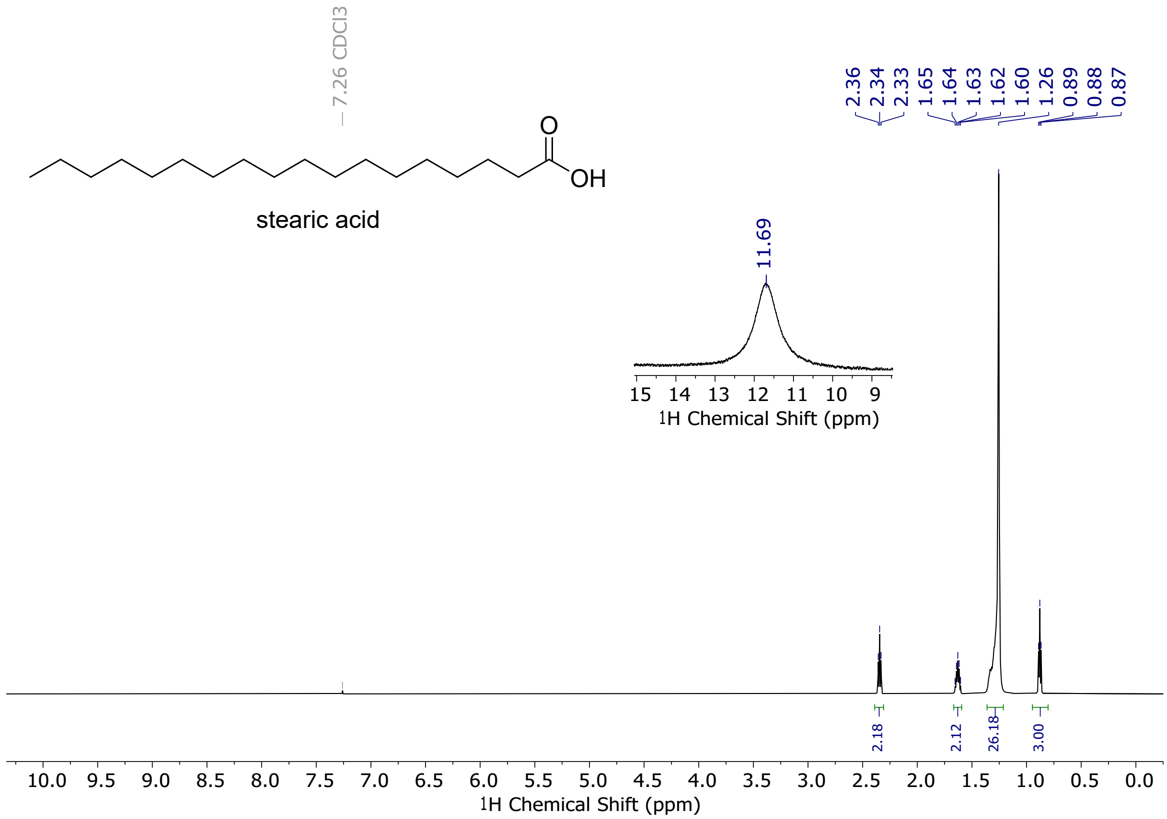
7.26 CDCl3
2.36
2.34
2.33
1.65
1.64
1.63
1.62
1.60
1.26
0.89
0.88
0.87
O
OH
stearic acid
11.69
15 14 13 12 11 10 9
1H Chemical Shift (ppm)
2.18
2.12
26.18
3.00
10.0 9.5 9.0 8.5 8.0 7.5 7.0 6.5 6.0 5.5 5.0 4.5 4.0 3.5 3.0 2.5 2.0 1.5 1.0 0.5 0.0
1H Chemical Shift (ppm)

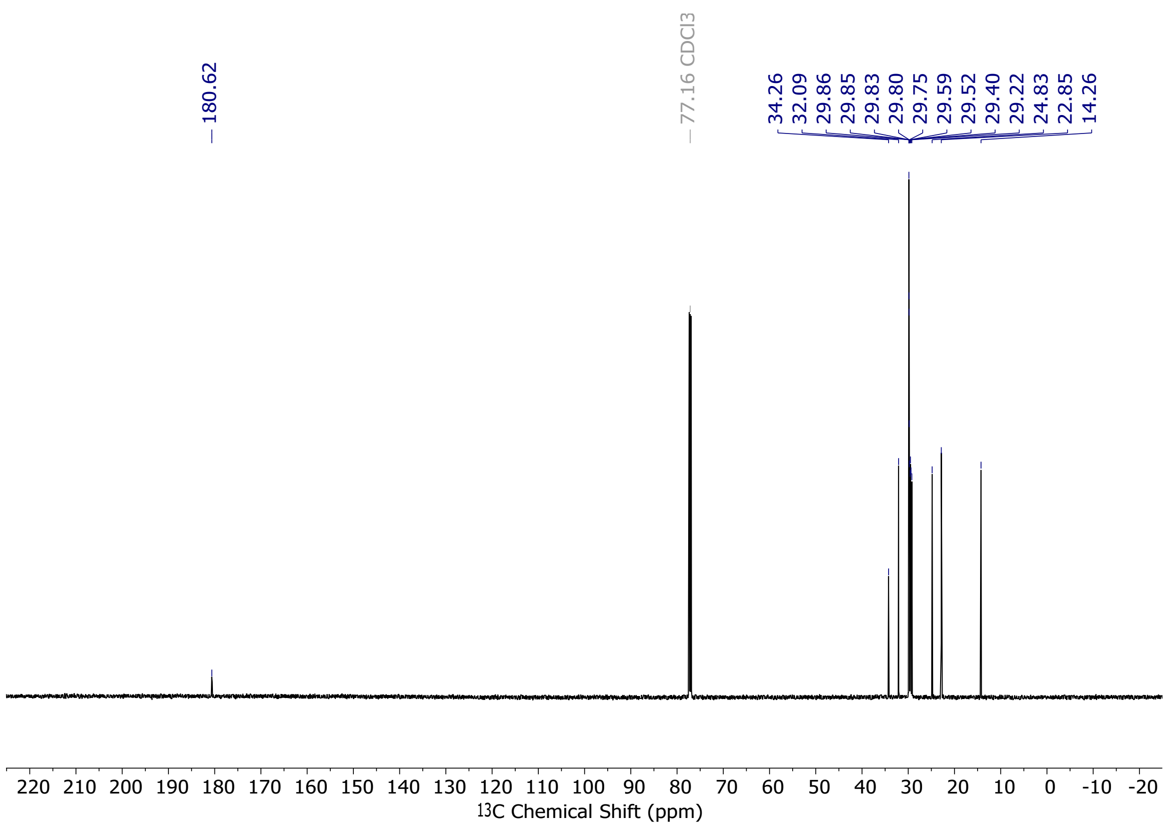
180.62
77.16 CDCl3
34.26
32.09
29.86
29.85
29.83
29.80
29.75
29.59
29.52
29.40
29.22
24.83
22.85
14.26
220 210 200 190 180 170 160 150 140 130 120 110 100 90 80 70 60 50 40 30 20 10 0 -10 -20
13C Chemical Shift (ppm)

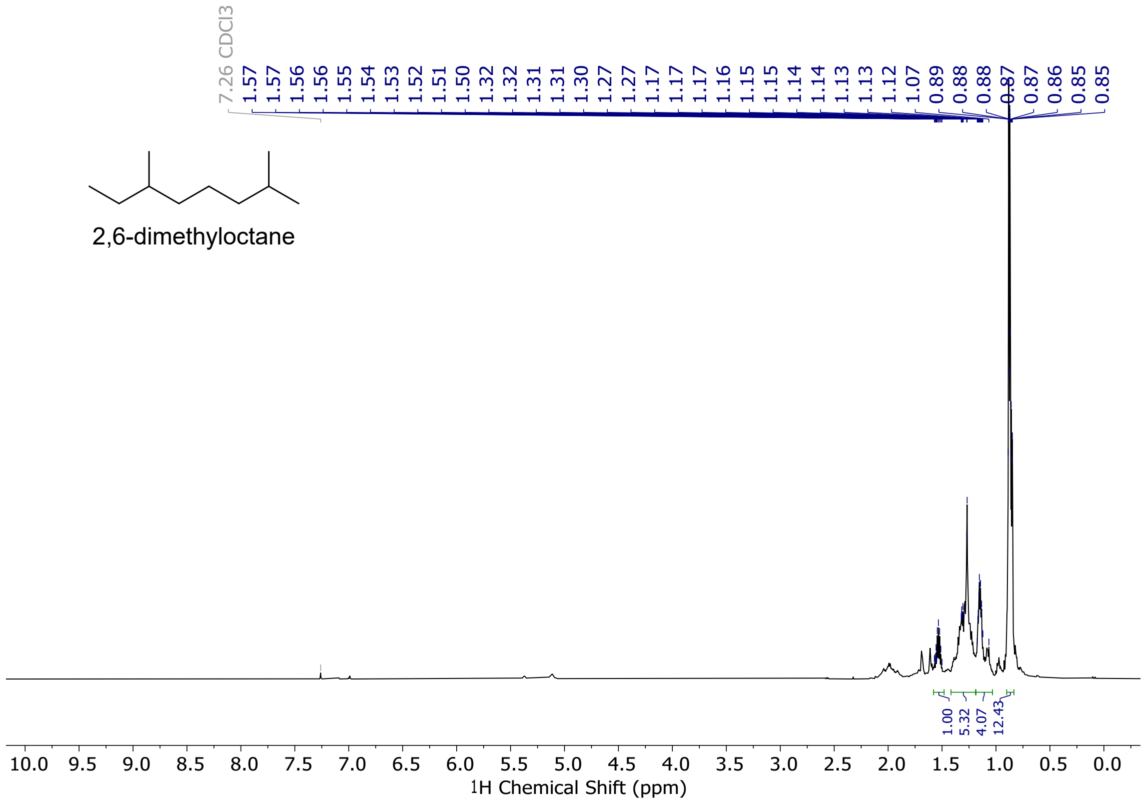
2,6-dimethyloctane
7.26 CDCl3
1.57 1.57 1.56 1.56 1.55 1.54 1.53 1.52 1.51 1.50 1.32 1.32 1.31 1.31 1.30 1.27 1.27 1.17 1.17 1.17 1.17 1.16 1.15 1.15 1.14 1.14 1.13 1.13 1.12 1.07 0.89 0.88 0.88 0.87 0.87 0.86 0.85 0.85
1.00
5.32
4.07
12.43
10.0 9.5 9.0 8.5 8.0 7.5 7.0 6.5 6.0 5.5 5.0 4.5 4.0 3.5 3.0 2.5 2.0 1.5 1.0 0.5 0.0
1H Chemical Shift (ppm)

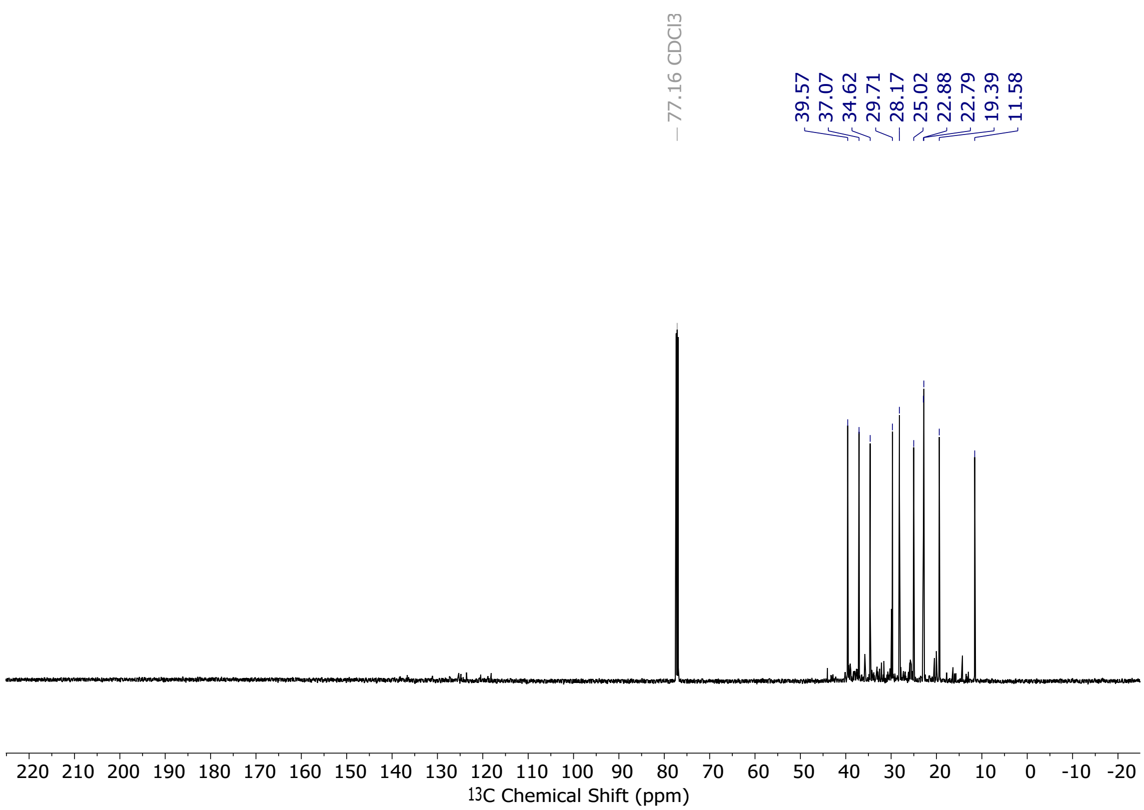
77.16 CDCl3
39.57 37.07 34.62 29.71 28.17 25.02 22.88 22.79 19.39 11.58
220 210 200 190 180 170 160 150 140 130 120 110 100 90 80 70 60 50 40 30 20 10 0 -10 -20
13C Chemical Shift (ppm)

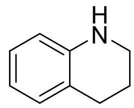

1,2,3,4-tetrahydroquinoline

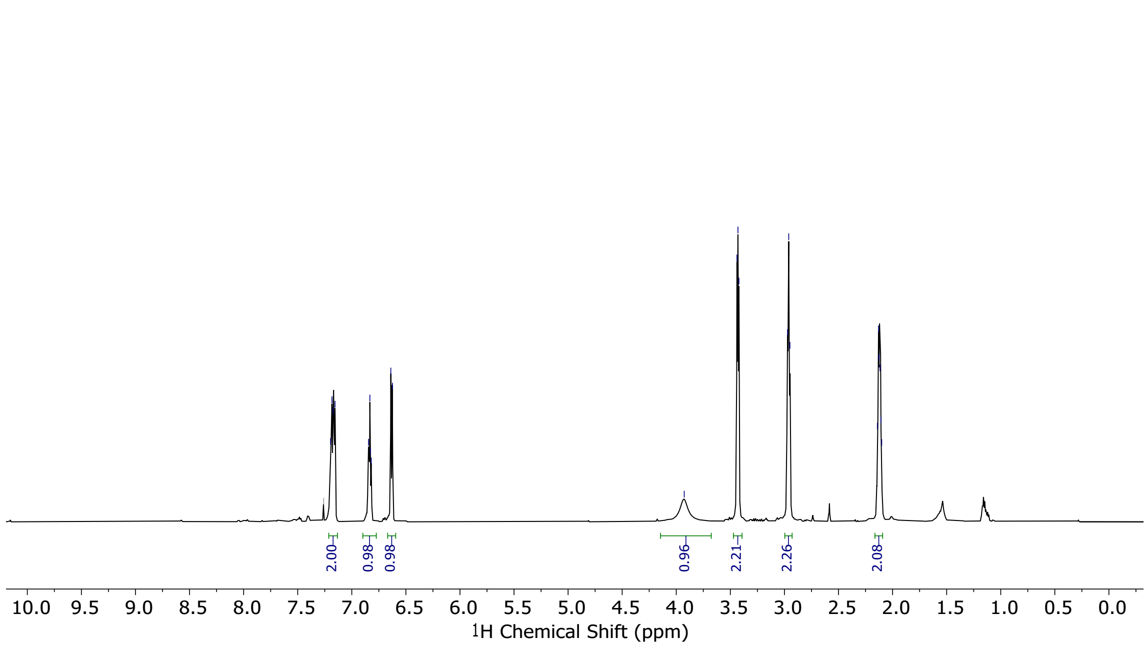

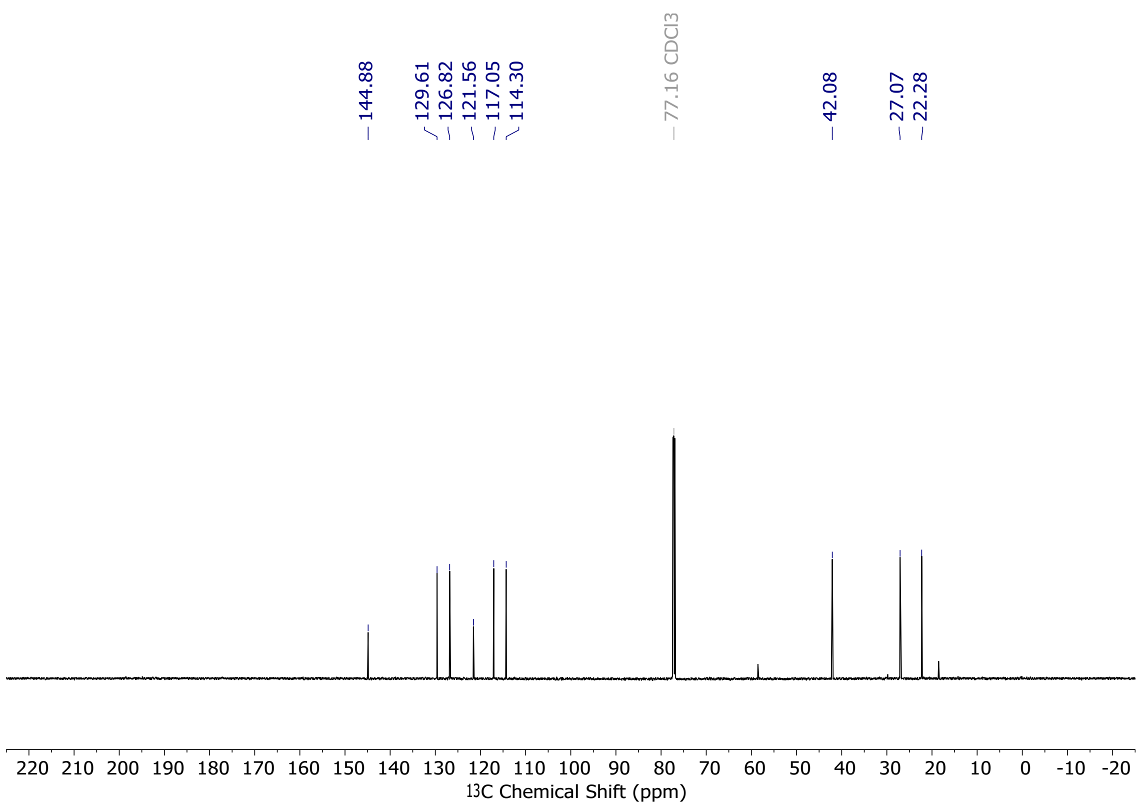

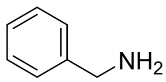

benzylamine

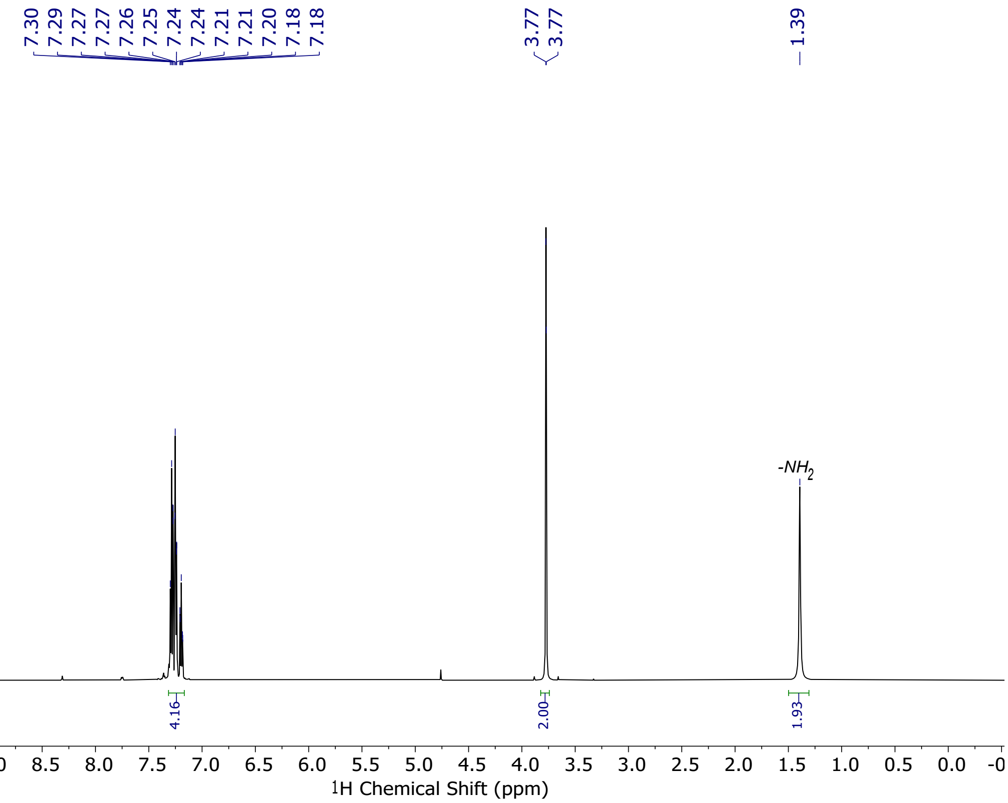

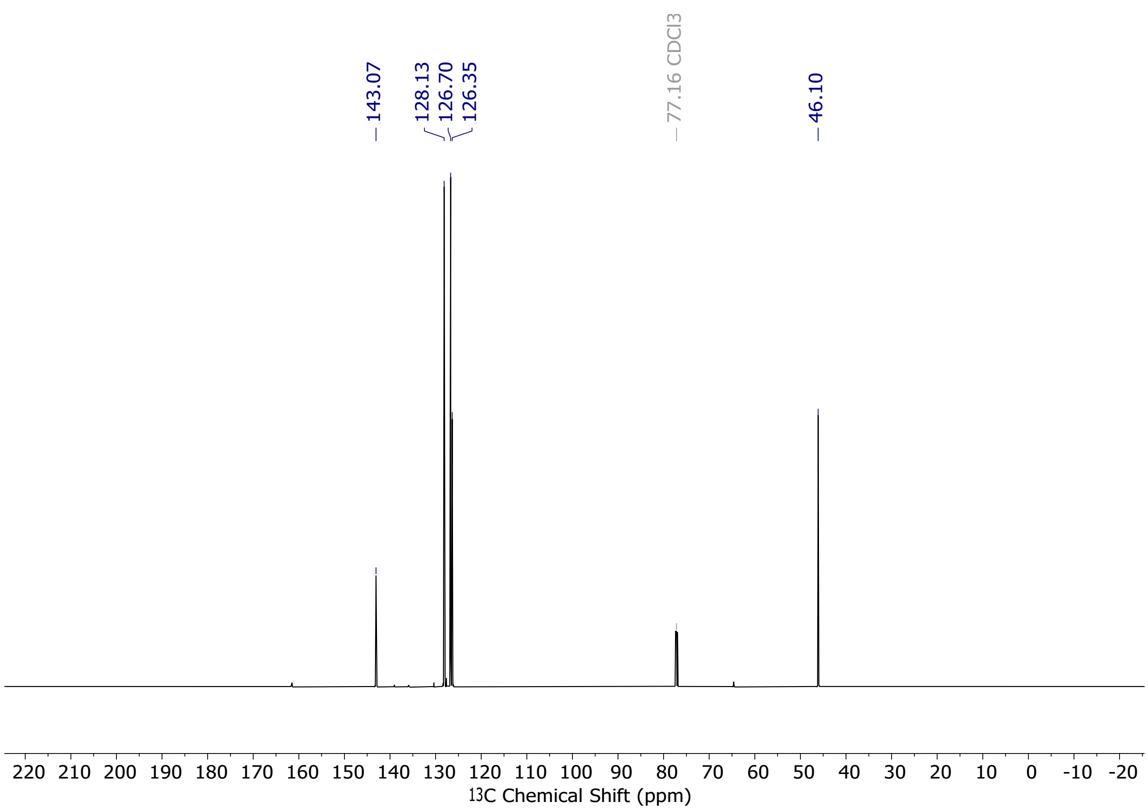

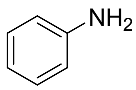
NH2

aniline

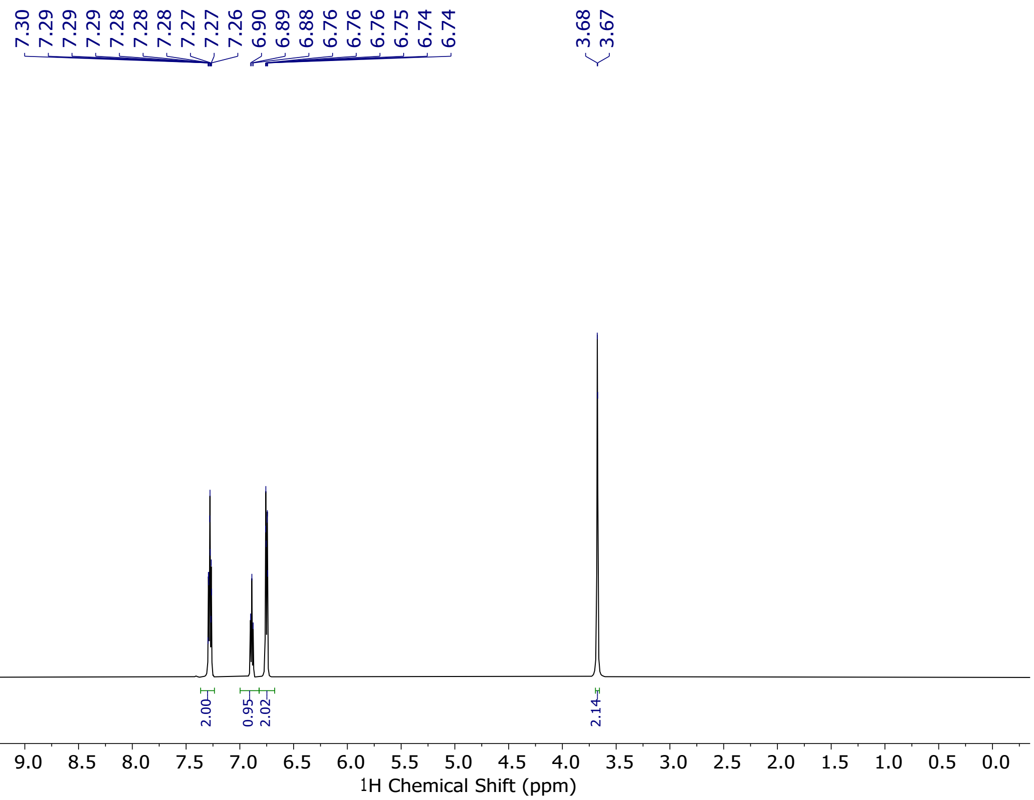
7.30
7.29
7.29
7.29
7.28
7.28
7.28
7.27
7.27
7.26
6.90
6.89
6.88
6.76
6.76
6.76
6.75
6.74
6.74
3.68
3.67
2.00
0.95
2.02
2.14
10.0 9.5 9.0 8.5 8.0 7.5 7.0 6.5 6.0 5.5 5.0 4.5 4.0 3.5 3.0 2.5 2.0 1.5 1.0 0.5 0.0
1H Chemical Shift (ppm)

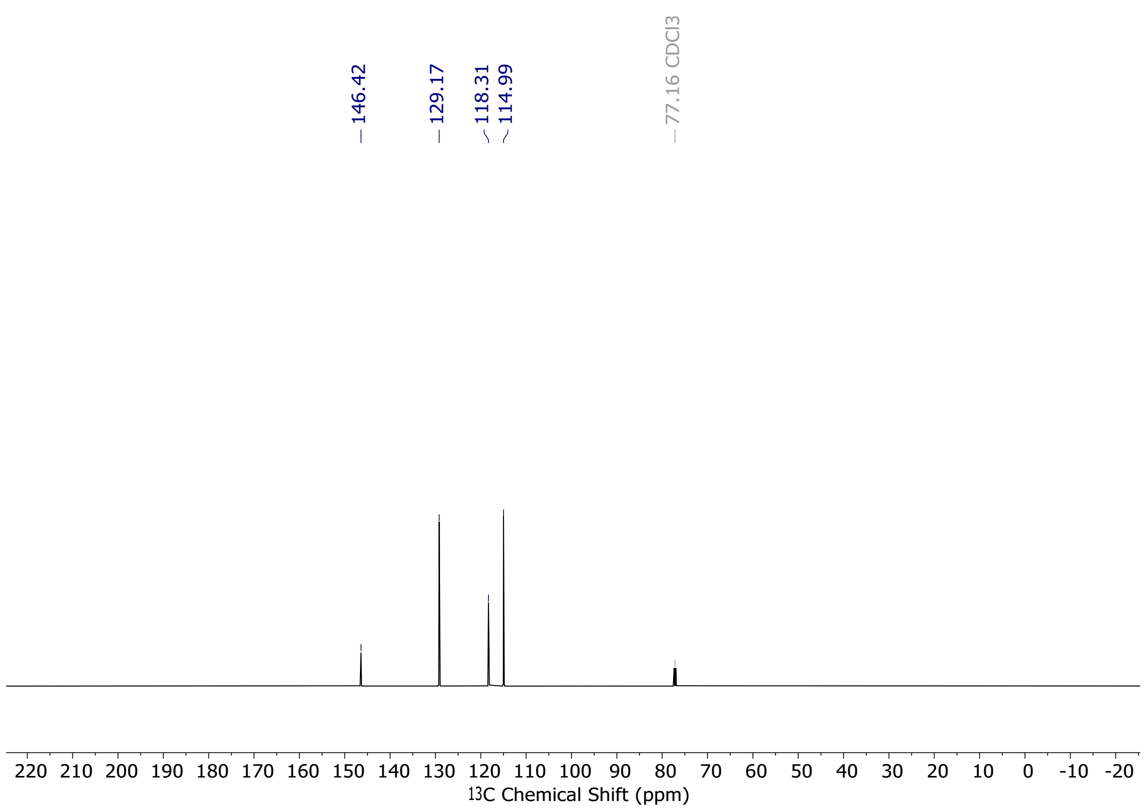
146.42
129.17
118.31
114.99
77.16 CDCl3
220 210 200 190 180 170 160 150 140 130 120 110 100 90 80 70 60 50 40 30 20 10 0 -10 -20
13C Chemical Shift (ppm)

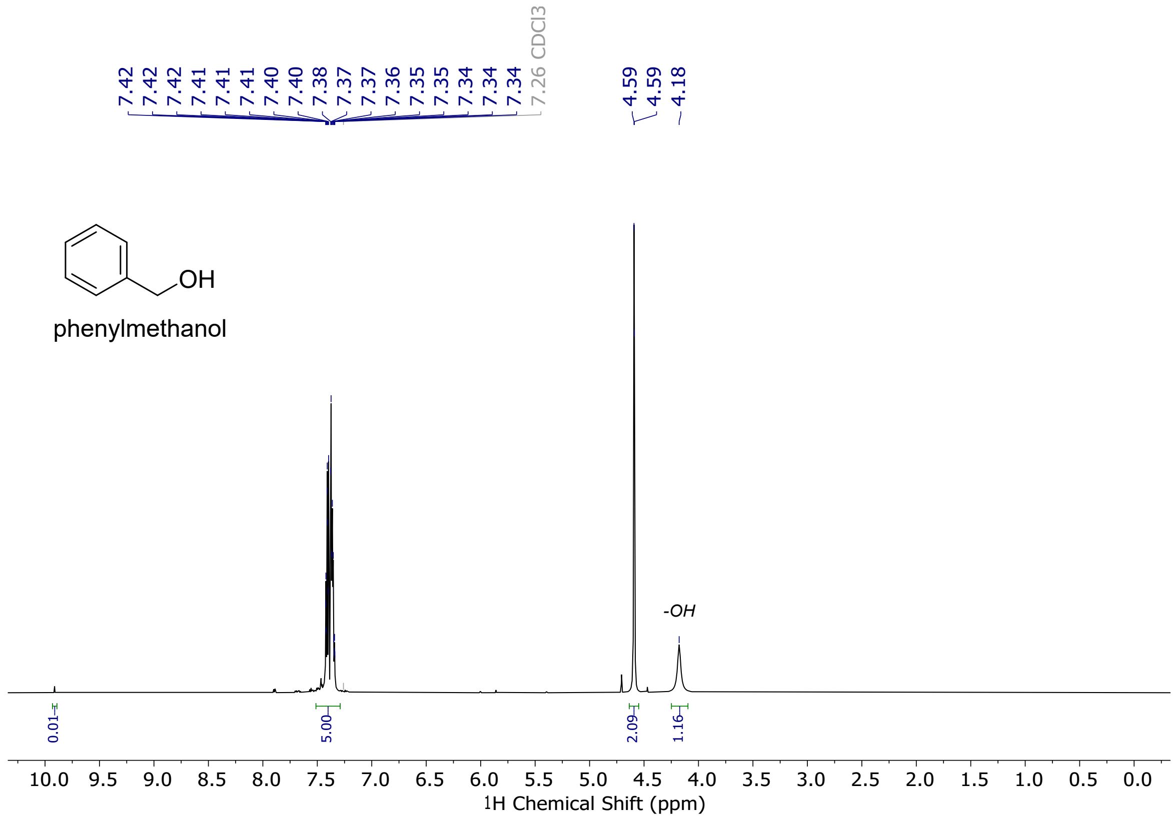
7.42
7.42
7.42
7.41
7.41
7.41
7.40
7.40
7.38
7.37
7.37
7.36
7.35
7.35
7.34
7.34
7.34
7.26 CDCl3
4.59
4.59
4.18
OH
phenylmethanol
-OH
0.01
5.00
2.09
1.16
10.0 9.5 9.0 8.5 8.0 7.5 7.0 6.5 6.0 5.5 5.0 4.5 4.0 3.5 3.0 2.5 2.0 1.5 1.0 0.5 0.0
1H Chemical Shift (ppm)

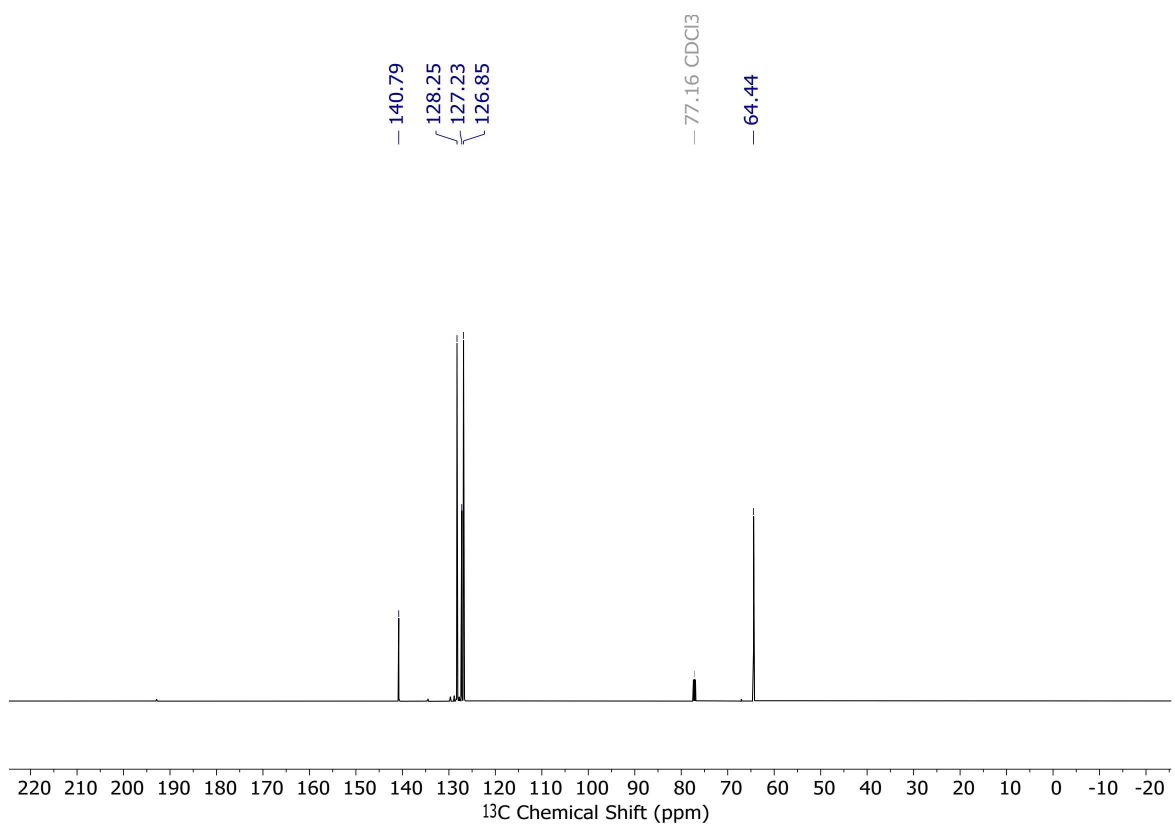
140.79
128.25
127.23
126.85
77.16 CDCl3
64.44
220 210 200 190 180 170 160 150 140 130 120 110 100 90 80 70 60 50 40 30 20 10 0 -10 -20
13C Chemical Shift (ppm)

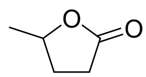

gamma valerolactone

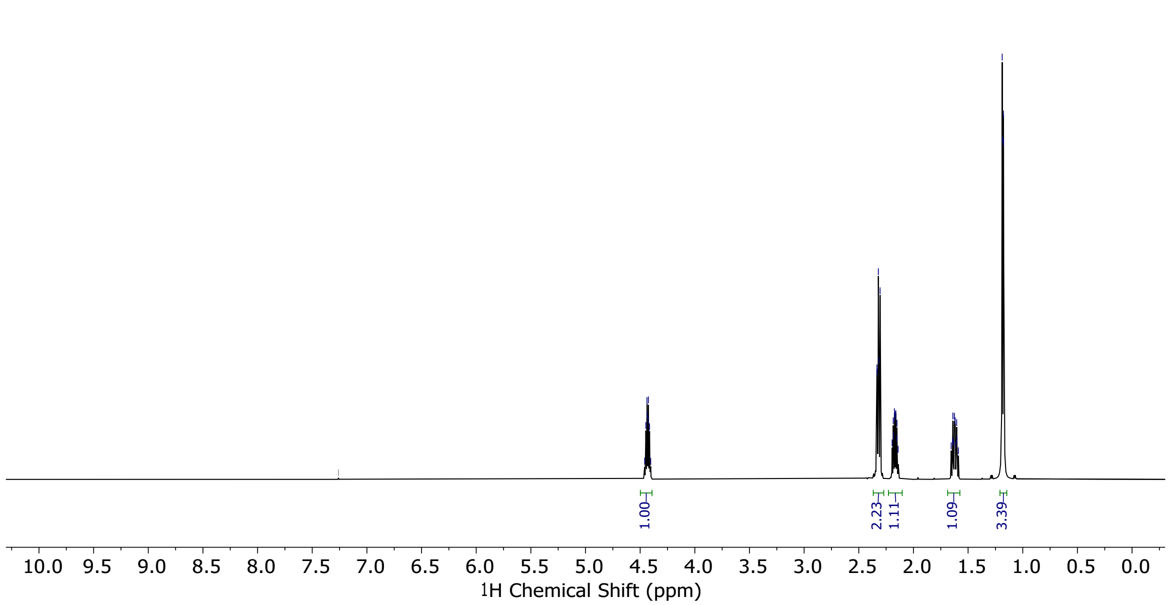

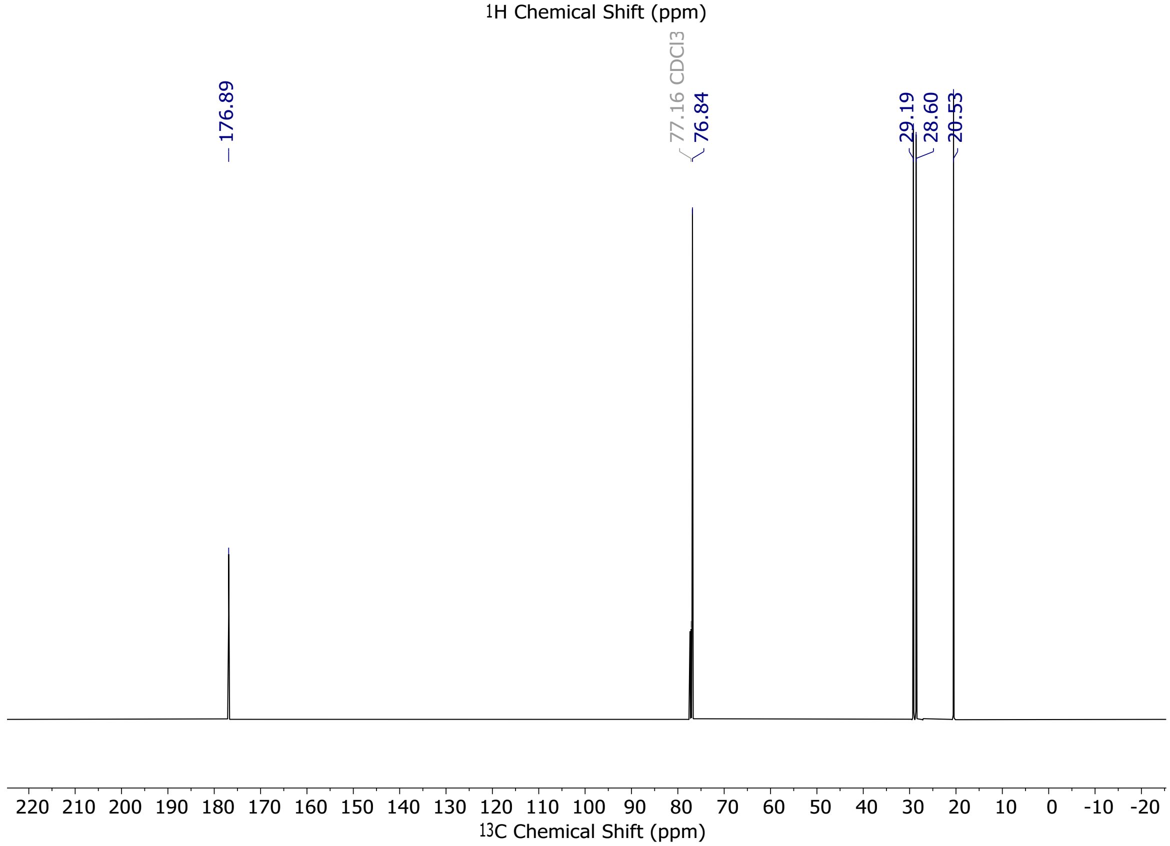

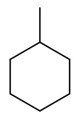

methylcyclohexane

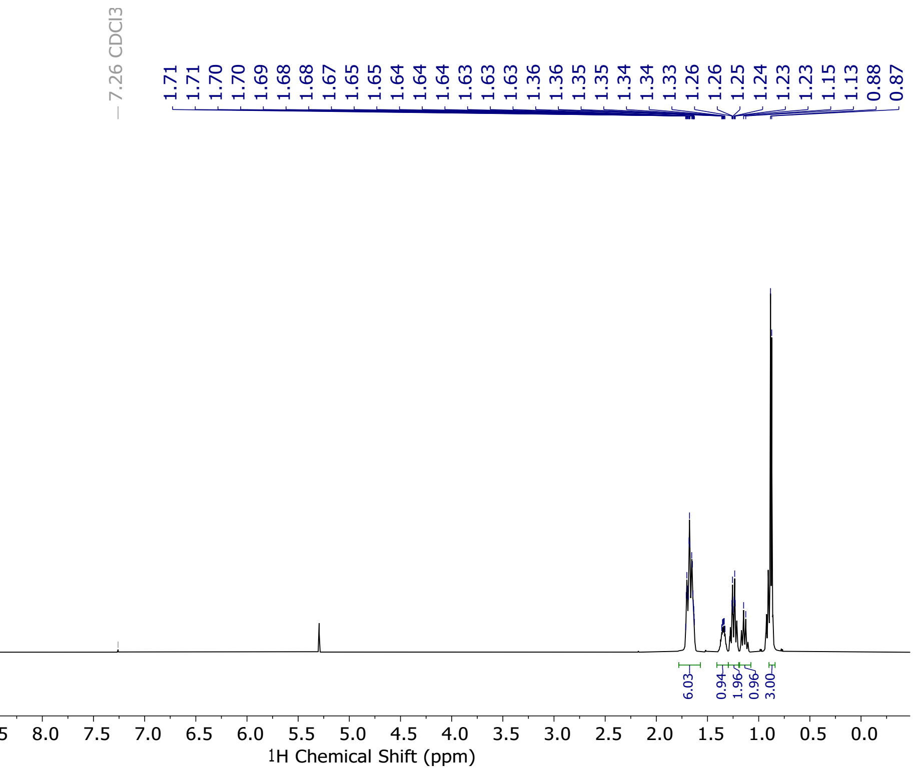

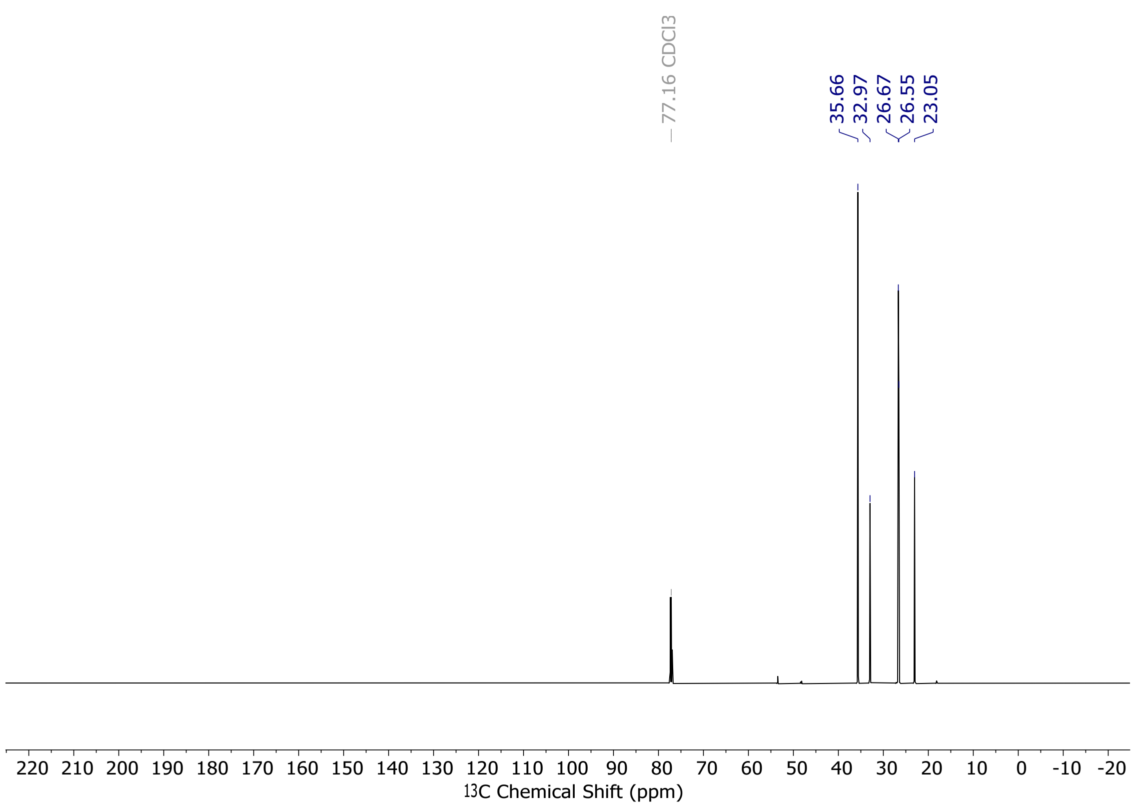

M. Bibliography

(1) Bergeret, G.; Gallezot, P. Particle Size and Dispersion Measurements. In *Handbook of Heterogeneous Catalysis*; John Wiley & Sons, Ltd, 2008; pp 738–765. https://doi.org/10.1002/9783527610044.hetcat0038.

(2) Serrano-Maldonado, A.; Bendounan, A.; Silly, M. G.; Pla, D.; Gómez, M. Selective Catalytic Hydrogenation of Fatty Acids with Cobalt–Halloysite Nanocomposites for Waste Valorization. *ACS Appl. Nano Mater.* **2023**, *6* (13), 11317–11326. https://doi.org/10.1021/acsanm.3c01361.

(3) Spies, P.; Schwendemann, S.; Lange, S.; Kehr, G.; Fröhlich, R.; Erker, G. Metal-Free Catalytic Hydrogenation of Enamines, Imines, and Conjugated Phosphinoalkenylboranes. *Angewandte Chemie International Edition* **2008**, *47* (39), 7543–7546. https://doi.org/10.1002/anie.200801432.

(4) Espinal-Viguri, M.; Neale, S. E.; Coles, N. T.; Macgregor, S. A.; Webster, R. L. Room Temperature Iron-Catalyzed Transfer Hydrogenation and Regioselective Deuteration of Carbon–Carbon Double Bonds. *J. Am. Chem. Soc.* **2019**, *141* (1), 572–582. https://doi.org/10.1021/jacs.8b11553.

(5) Pérez Alonso, A.; Mauriés, S.; Ledeuil, J.-B.; Madec, L.; Pham Minh, D.; Pla, D.; Gómez, M. Nickel Nanoparticles Immobilized on Pristine Halloysite: An Outstanding Catalyst for Hydrogenation Processes. *ChemCatChem* **2022**, *14* (22), e202200775. https://doi.org/10.1002/cctc.202200775.

(6) Udayakumar, V.; Pandurangan, A. A Novel Route for the Synthesis of Alkanes from Glycerol in a Two Step Process Using a Pd/SBA-15 Catalyst. *RSC Adv.* **2015**, *5* (96), 78719–78727. https://doi.org/10.1039/C5RA10744J.

(7) Pulido-Díaz, I. T.; Serrano-Maldonado, A.; López-Suárez, C. C.; Méndez-Ocampo, P. A.; Portales-Martínez, B.; Gutiérrez-Alejandre, A.; Salas-Martin, K. P.; Guerrero-Ríos, I. RhNPs Supported on *N* -Functionalized Mesoporous Silica: Effect on Catalyst Stabilization and Catalytic Activity. *Dalton Trans.* **2021**, *50* (9), 3289–3298. https://doi.org/10.1039/D0DT04213G.